

# Nuclear models for inclusive and semi-inclusive neutrino reactions in Carbon, Oxygen and Argon

**Maria B. Barbaro**

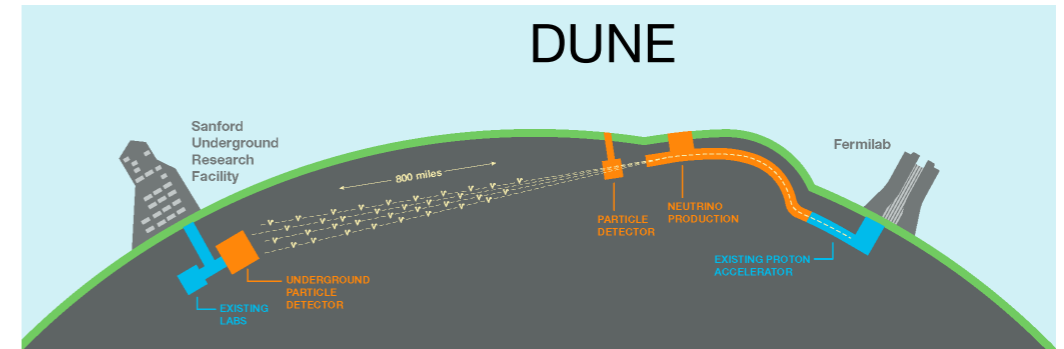
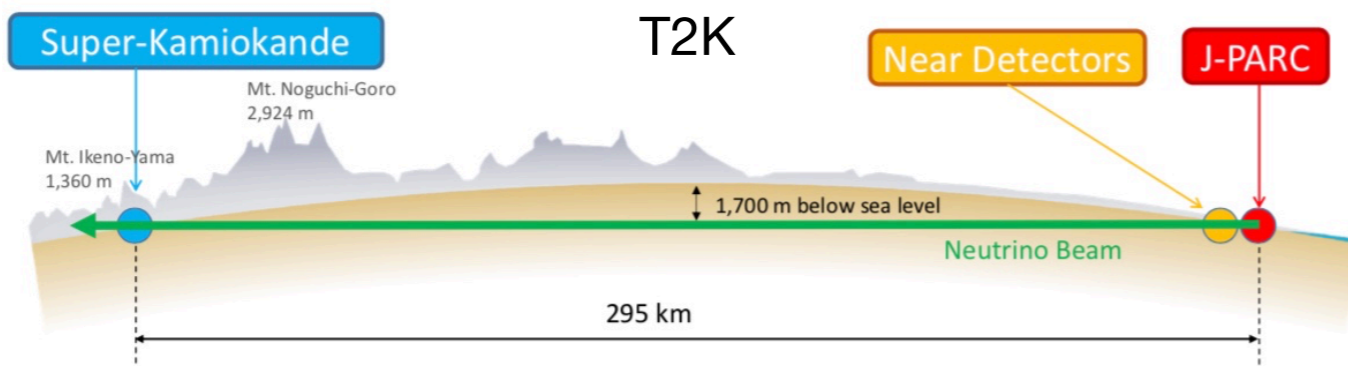
**University of Turin and INFN  
IJCLab, Orsay**



**P2IO/BSM First Workshop  
February 11-12, 2021**

# Nuclear physics for neutrino physics: neutrino oscillation experiments

Nuclear models are necessary for the interpretation of long baseline neutrino experiments in search of BSM physics: leptonic CP violation, improved accuracy on oscillation angles, neutrino mass ordering



The extraction of the oscillation parameters in the neutrino mixing matrix  $U$  from the measurement of oscillation probabilities crucially depends on the accurate knowledge of the neutrino energy

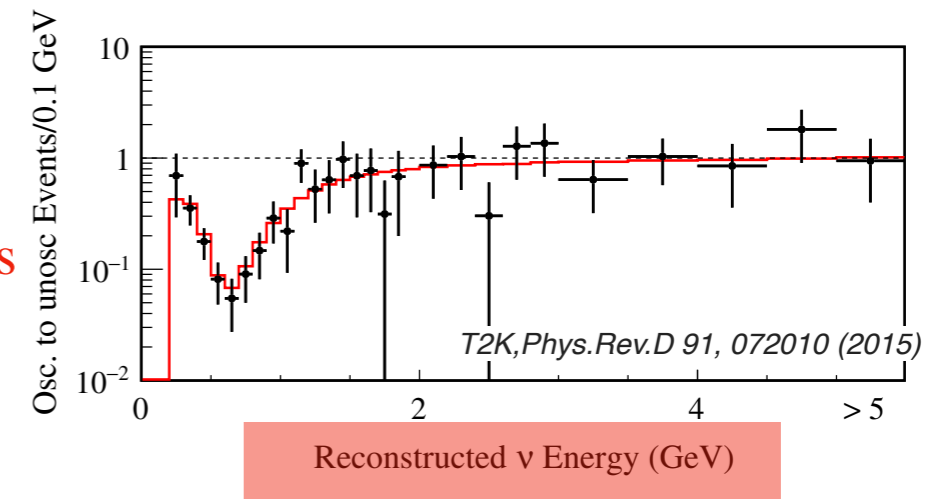
$$P_{\alpha \rightarrow \beta} = \left| \langle \nu_{\alpha} | \nu_{\beta}(t) \rangle \right|^2 = \left| \sum_i U_{\alpha i}^* U_{\beta i} e^{im_i^2 L/2E_{\nu}} \right|^2$$

$E_{\nu}$  must be reconstructed from the kinematics of the detected particles (leptons, nucleons, pions...)

Detectors are made of **complex nuclei** (C, O, Ar,...): reliable nuclear models are needed for data analyses.

Large systematic uncertainty from modeling of neutrino-nucleus interactions.

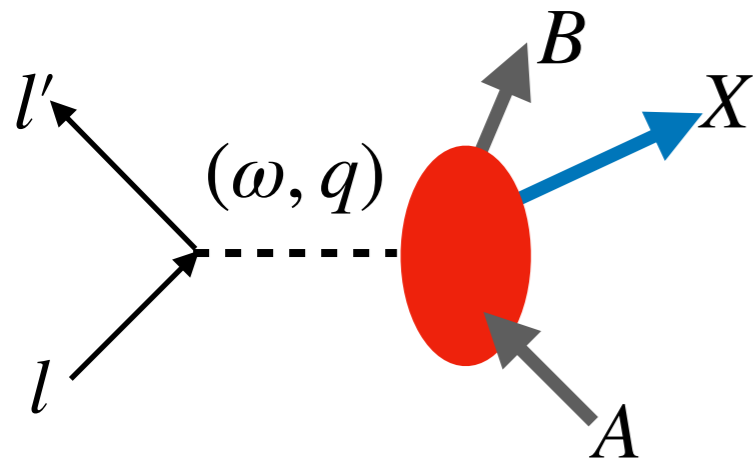
**The success of future experiments largely relies on the ability to reduce this uncertainty.**



Type of Uncertainty	$\nu_e/\bar{\nu}_e$ Candidate Relative Uncertainty (%)
Super-K Detector Model	1.5
Pion Final State Interaction and Rescattering Model	1.6
Neutrino Production and Interaction Model Constrained by ND280 Data	2.7
Electron Neutrino and Antineutrino Interaction Model	3.0
Nucleon Removal Energy in Interaction Model	3.7
Modeling of Neutral Current Interactions with Single $\gamma$ Production	1.5
Modeling of Other Neutral Current Interactions	0.2
Total Systematic Uncertainty	6.0

T2K, Nature 580 (2020)

# Nuclear response to a electroweak probe



$$l(A, BX)l'$$

**Inclusive** measurement

(only the final lepton is observed)

$$l(A, B)Xl'$$

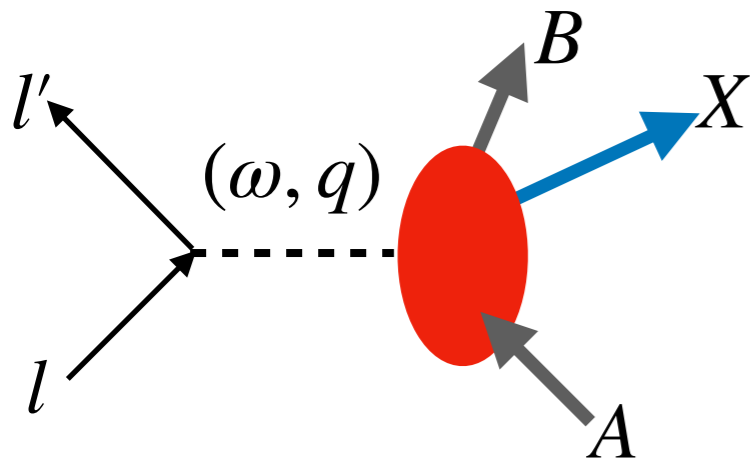
**Exclusive** or **semi-inclusive** measurement

(the final lepton is detected in coincidence with one or more other reaction products, *e.g.* a proton)

Strict analogy between neutrino ( $W^\pm, Z^0$  exchange) and electron (mainly  $\gamma$  exchange) scattering:

the vector currents are related by an isospin rotation and the effects of the nuclear medium are expected to be the same.

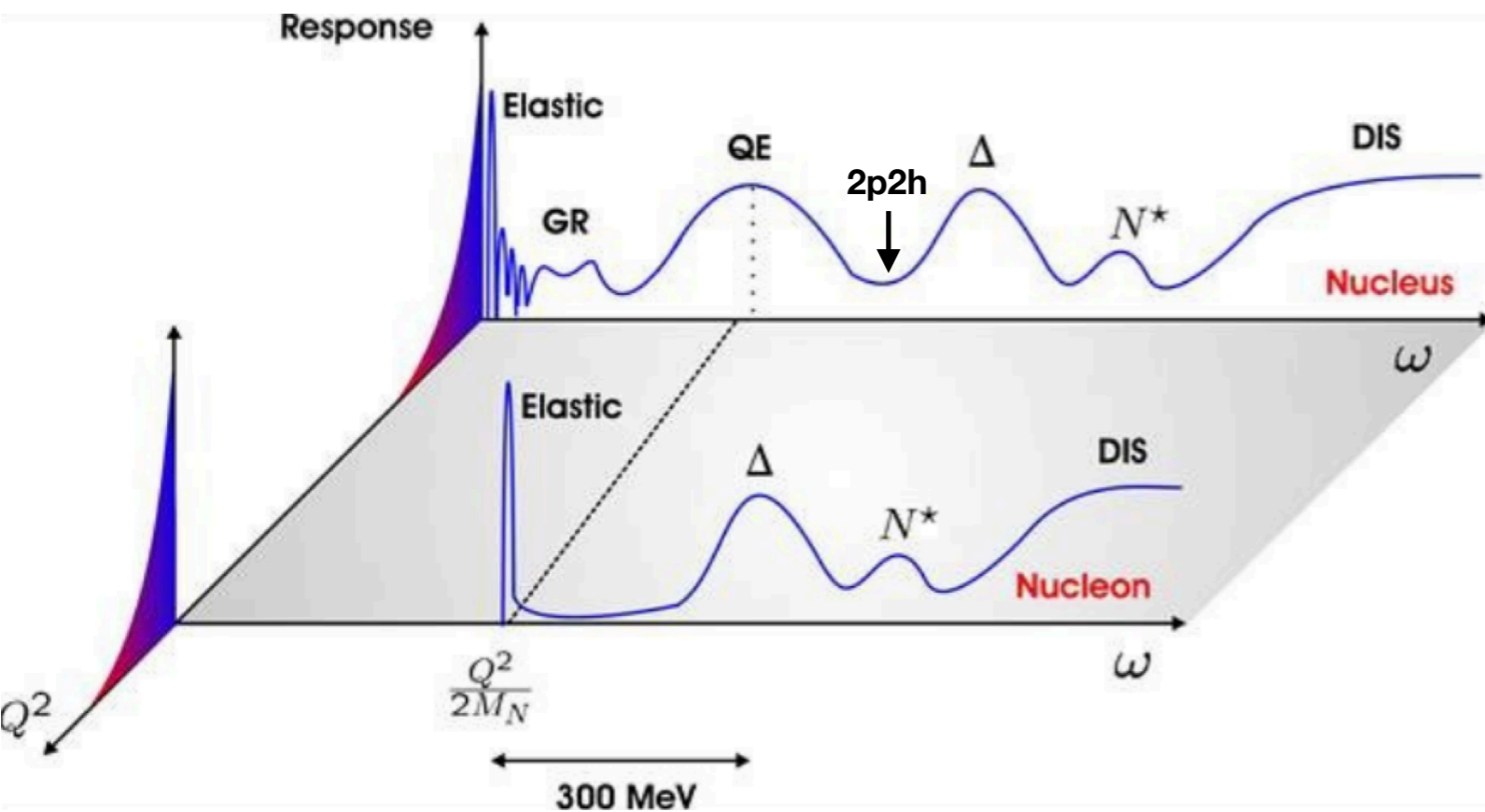
# Nuclear response to a electroweak probe



$l(A, BX)l'$  **Inclusive** measurement  
(only the final lepton is observed)

$l(A, B)Xl'$  **Exclusive or semi-inclusive** measurement  
(the final lepton is detected in coincidence with one or more other reaction products, e.g. a proton)

Strict analogy between neutrino ( $W^\pm, Z^0$  exchange) and electron (mainly  $\gamma$  exchange) scattering:  
the vector currents are related by an isospin rotation and the effects of the nuclear medium are expected to be the same.



$$\begin{aligned} \omega &= \varepsilon' - \varepsilon && \text{energy transfer} \\ \mathbf{q} &= \mathbf{k} - \mathbf{k}' && \text{momentum transfer} \\ Q^2 &= q^2 - \omega^2 && \text{four-momentum transfer} \end{aligned}$$

variables commonly used in electron scattering studies, where they can be precisely measured. In neutrino experiments the incoming energy is not exactly known: cross sections must be averaged over the **neutrino flux**  $\Phi(E_\nu)$   
->  **$\omega$  and  $q$  are not accessible**

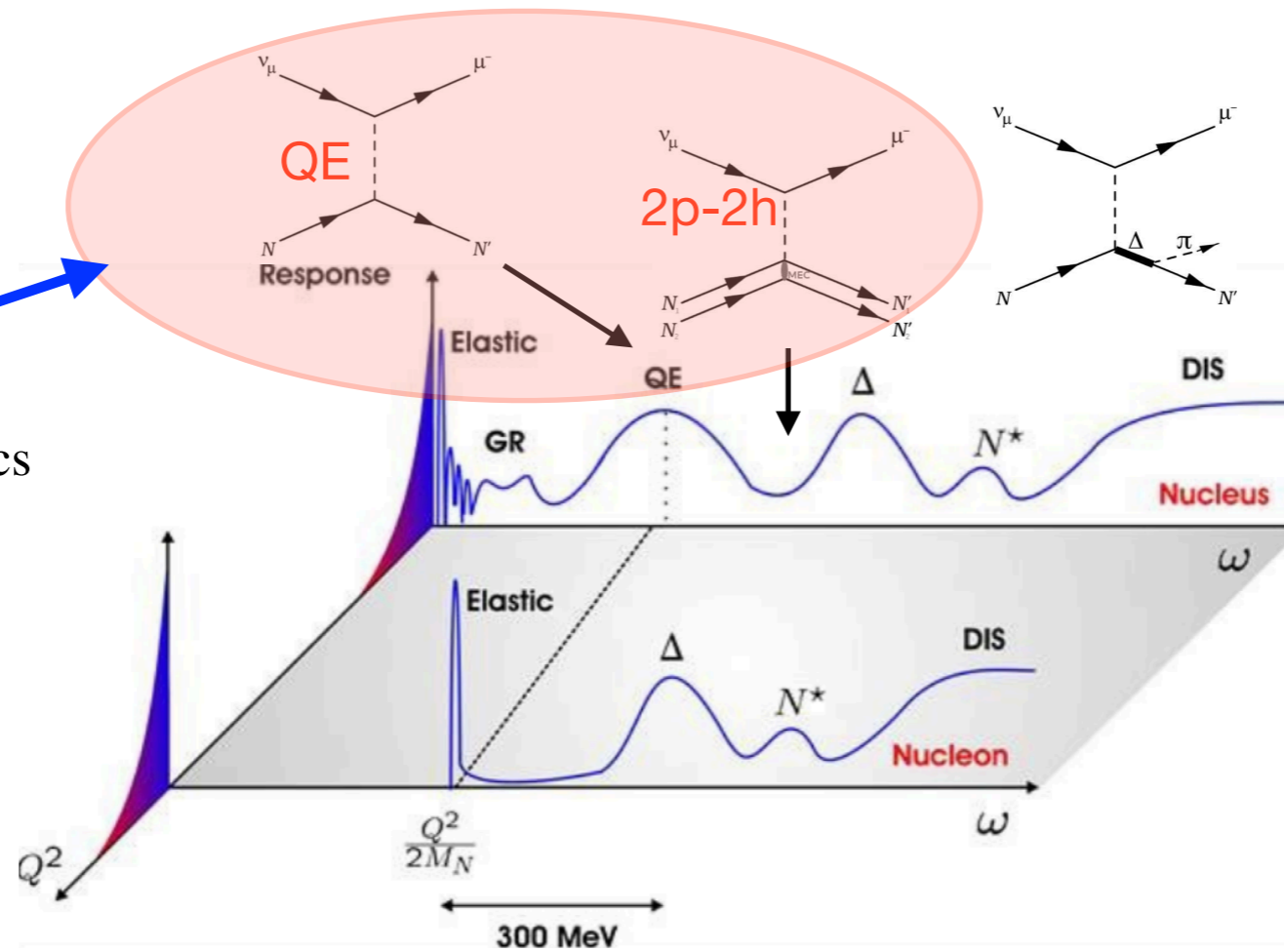
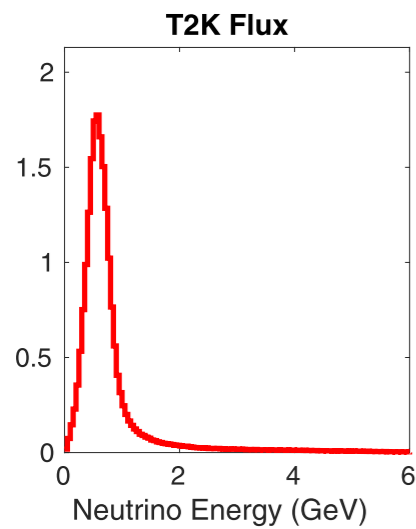
$$\frac{d^2\sigma}{dT_\mu d \cos \theta_\mu} = \frac{1}{\Phi_{tot}} \int \left[ \frac{d^2\sigma}{dT_\mu d \cos \theta_\mu} \right]_{E_\nu} \Phi(E_\nu) dE_\nu$$

Different processes, from low energy collective excitations up to deep inelastic scattering at high energies, can contribute to the same final lepton kinematics and cannot be disentangled: multiscale problem.

The goal of Monte Carlo **event generators** (GENIE, NEUT, NuWro, GIBUU) is to model all these reactions.

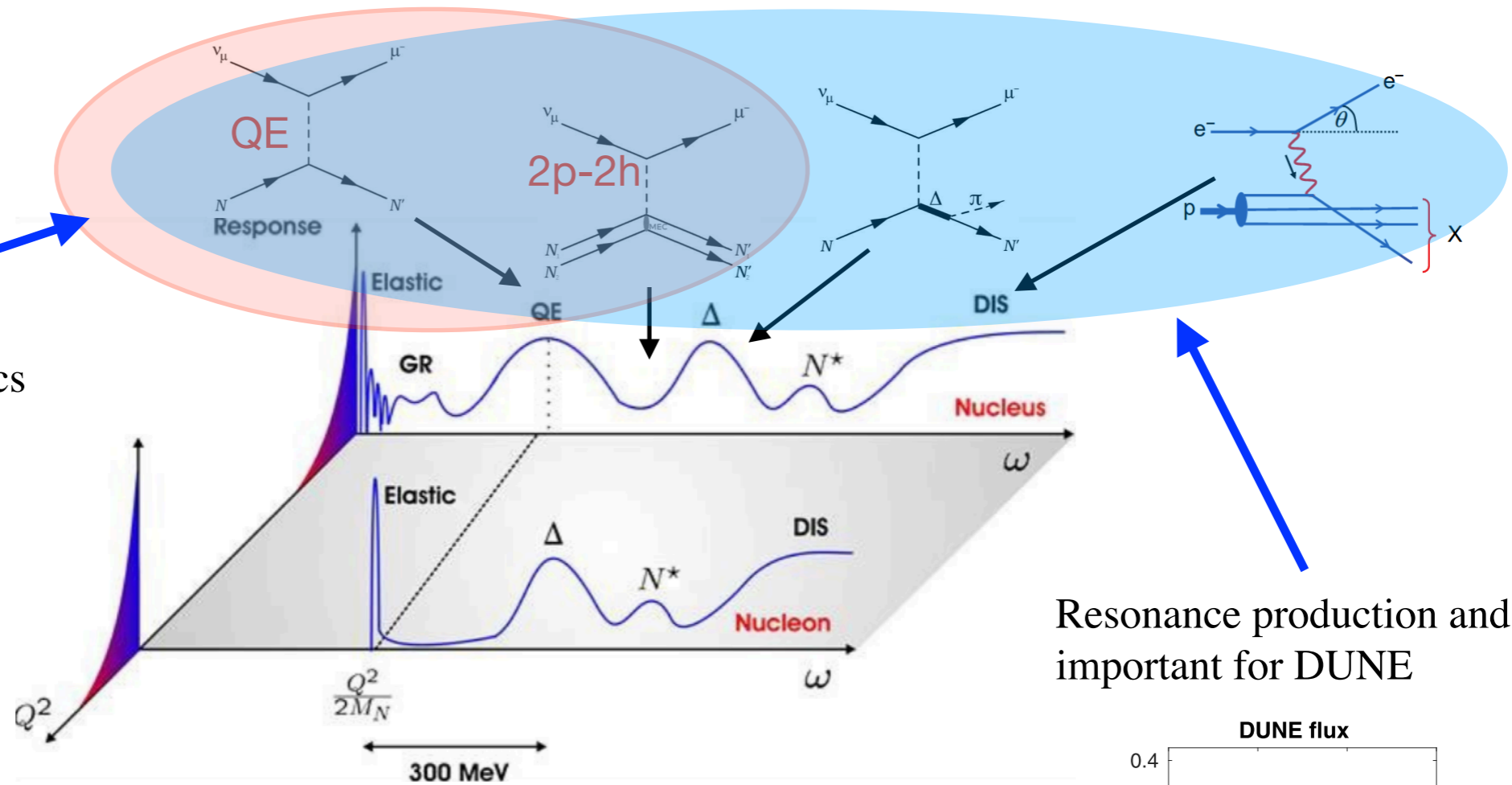
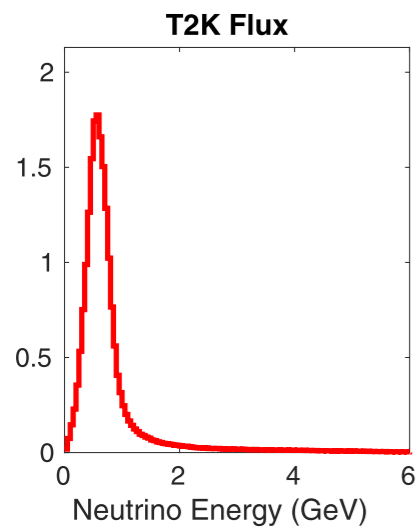
# Nuclear response to electroweak probes

QE and 2p2h dominant at T2K kinematics

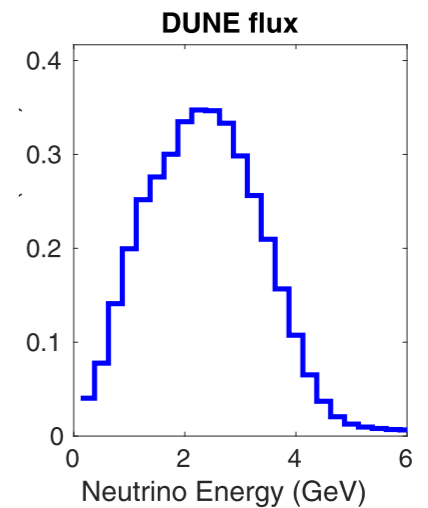


# Nuclear response to electroweak probes

QE and 2p2h dominant at T2K kinematics



Resonance production and DIS important for DUNE



Basic requirements for a “good” nuclear model to be used in neutrino oscillation analyses:

- ☑ **relativistic** (the relevant energies belong to the GeV regime)
- ☑ **compare well with existing electron scattering data**
- ☑ **implementable in Monte Carlo generators**
- ☐ **consistent** description of the full spectrum covered by the  $\nu$  flux (the most challenging)

Intense theoretical activity in the last ~10-15 years aiming at improved description of nuclear effects in different energy regions within various theoretical frameworks:

- ▶ RPA and HF-RPA: Lyon/Paris (Martini and Ericson), Valencia (Nieves and coll.), Gent (Jachowicz and coll.)
- ▶ Spectral function approach (Rome, Benhar and coll.)
- ▶ Relativistic Green’s function (Pavia, Giusti and coll.)
- ▶ “Ab initio” (Los Alamos, Lovato and coll.)
- ▶ Superscaling “SuSA” approach (MIT, Torino, Sevilla, Granada, Madrid)

.....

see [NuSTEC White Paper](#) for an (almost) up-to-date review:

L.Alvarez-Ruso *et al.*, Prog.Part.Nucl.Phys. 100 (2018)

Almost all papers up to now have been focussed on **inclusive** reactions.

More work on **semi-inclusive** is needed to better constrain nuclear models.

# Formalism

Double differential neutrino (+) or antineutrino (-) Charged Current cross section on a nucleus

**Inclusive** case: only the final lepton is detected, e.g.  $(\nu_\mu, \mu)$

$$\left[ \frac{d\sigma}{dk_\mu d\Omega_\mu} \right]_{\pm} = \sigma_0 \mathcal{F}_{\pm}^2 \sim \eta_{\mu\nu} W^{\mu\nu}$$

$$\sigma_0 = \frac{G_F^4 \cos^2 \theta_C}{2\pi^2} \left( k_\mu \cos \frac{\tilde{\theta}_\mu}{2} \right)^2$$

$\eta_{\mu\nu}$  **leptonic tensor**

$$W^{\mu\nu} = \sum \delta(E_f - E_i - \omega) \langle f | J^\mu(Q) | i \rangle^* \langle f | J^\nu(Q) | i \rangle$$

**hadronic tensor**

$J^\mu = J_V^\mu + J_A^\mu$  nuclear current,  $|i, f\rangle$  nuclear states

$$\mathcal{F}_{\pm}^2 = V_{CC} R_{CC} + 2V_{CL} R_{CL} + V_{LL} R_{LL} + V_T R_T \pm V_{T'} R_{T'} \quad \text{embodies the nuclear dynamics}$$

Rosenbluth-like separation  $\mathbf{q} // \hat{\mathbf{z}}$ : **5 response functions**

$$R_K = R_K^{VV} + R_K^{AA}, \quad K = CC, CL, LL, T \quad R_K \equiv R_K(q, \omega)$$

$$R_{T'} = R_{T'}^{VA}$$

Each response is a component of the hadronic tensor  $W^{\mu\nu}$  and depends on two independent variables  $(q, \omega)$

Comparison with electron scattering  $(e, e')$

$$\frac{d\sigma}{dk_e d\Omega_e} = \sigma_{Mott} (v_L R_L^{VV} + v_T R_T^{VV}) \quad \text{only 2 vector responses}$$

**Semi-inclusive** case  $(\nu_l, lN)$ : 10 responses, 5 variables



# Quasielastic region and SuperScaling

Many high quality **electron scattering** data can be used not only as a **test** but also as an **input** for neutrino cross sections [Amaro *et al.*, PRC71 (2005)]. The “Superscaling” behaviour emerges from the analysis of  $(e,e')$  data in the quasielastic region.

**SuperScaling  
function**

$$f(q, \omega; k_F) = k_F \times \frac{\left[ d^2\sigma/d\omega d\Omega_e \right]_{exp} \quad q \gtrsim 300 \text{ MeV}/c}{\bar{\sigma}_{eN}(q, \omega; p = p_{min}, \mathcal{E} = 0)} \longrightarrow f(\psi)$$

embodies  
nuclear  
effects

**Scaling variable**  $\psi \equiv \psi(q, \omega)$  - or  $y(q, \omega)$  - is a specific combination of the two variables  $q$  and  $\omega$  (analogous to  $x$  in DIS)

# Quasielastic region and SuperScaling

Many high quality **electron scattering** data can be used not only as a **test** but also as an **input** for neutrino cross sections [Amaro *et al.*, PRC71 (2005)]. The “Superscaling” behaviour emerges from the analysis of  $(e,e')$  data in the quasielastic region.

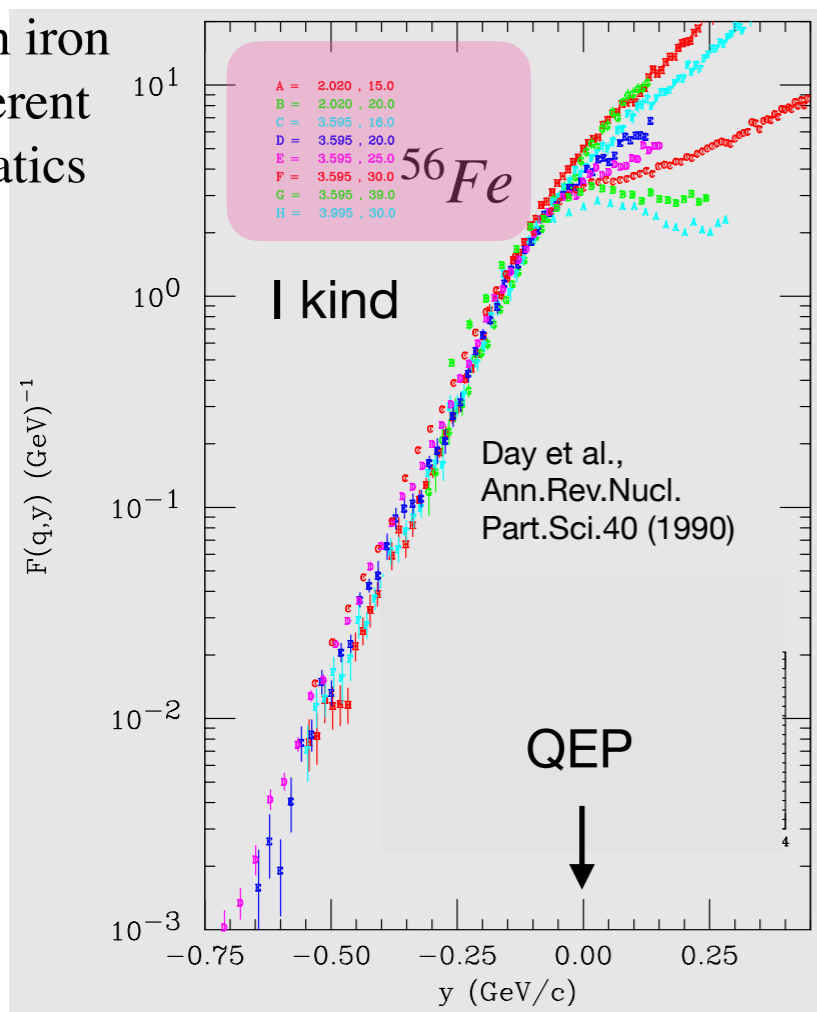
**SuperScaling function**

$$f(q, \omega; k_F) = k_F \times \frac{[d^2\sigma/d\omega d\Omega_e]_{exp} \quad q \gtrsim 300 \text{ MeV}/c}{\bar{\sigma}_{eN}(q, \omega; p = p_{min}, \mathcal{E} = 0)} \longrightarrow f(\psi)$$

embodies nuclear effects

**Scaling variable**  $\psi \equiv \psi(q, \omega)$  - or  $y(q, \omega)$  - is a specific combination of the two variables  $q$  and  $\omega$  (analogous to  $x$  in DIS)

data on iron at different kinematics



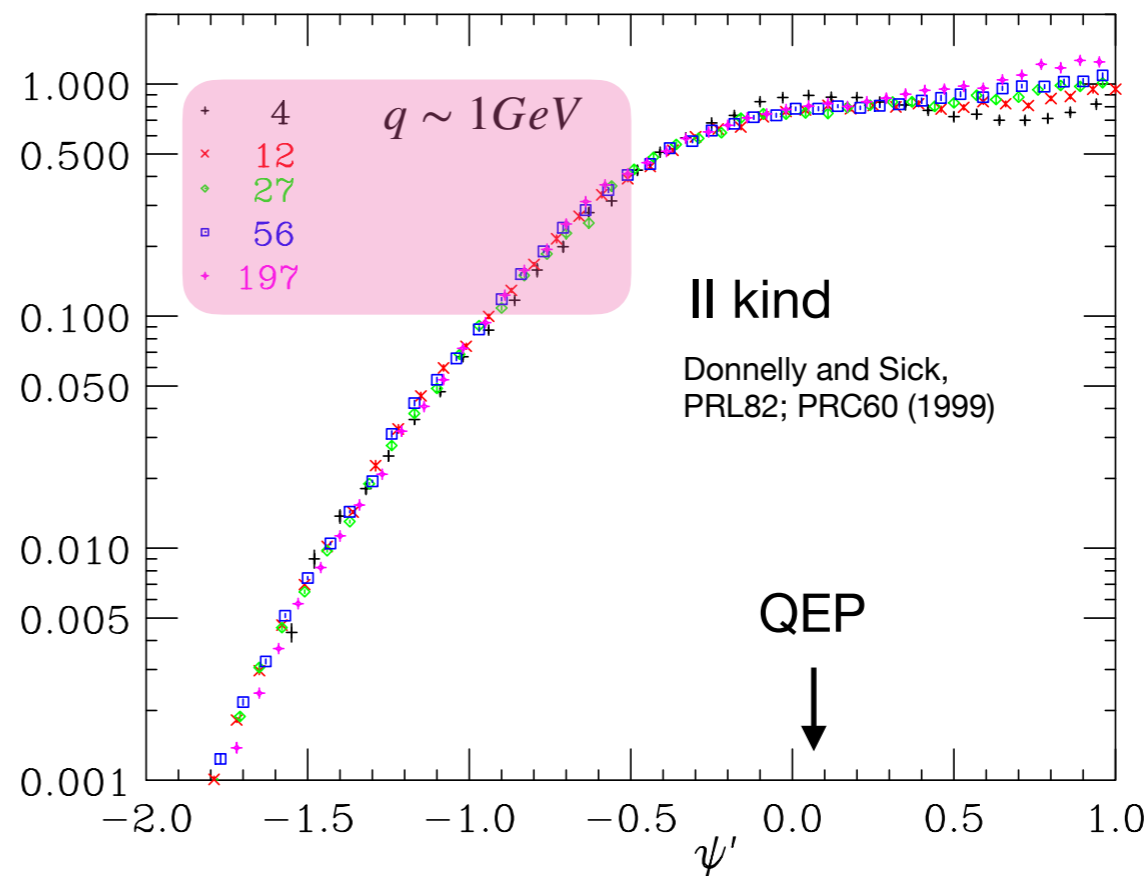
**Scaling of first kind:**

$$f(q, \omega; k_F) \rightarrow f(\psi; k_F)$$

**no dependence on kinematics**

**for a specific nucleus**

$f(\psi')$



data on different nuclei at fixed kinematics

**Scaling of second kind:  $f(\psi; k_F) \rightarrow f(\psi)$**

**no dependence on the nuclear species**

**at fixed kinematics**

**I+II kind = SuperScaling**

# Quasielastic region and SuperScaling

Many high quality **electron scattering** data can be used not only as a **test** but also as an **input** for neutrino cross sections [Amaro *et al.*, PRC71 (2005)]. The “Superscaling” behaviour emerges from the analysis of  $(e,e')$  data in the quasielastic region.

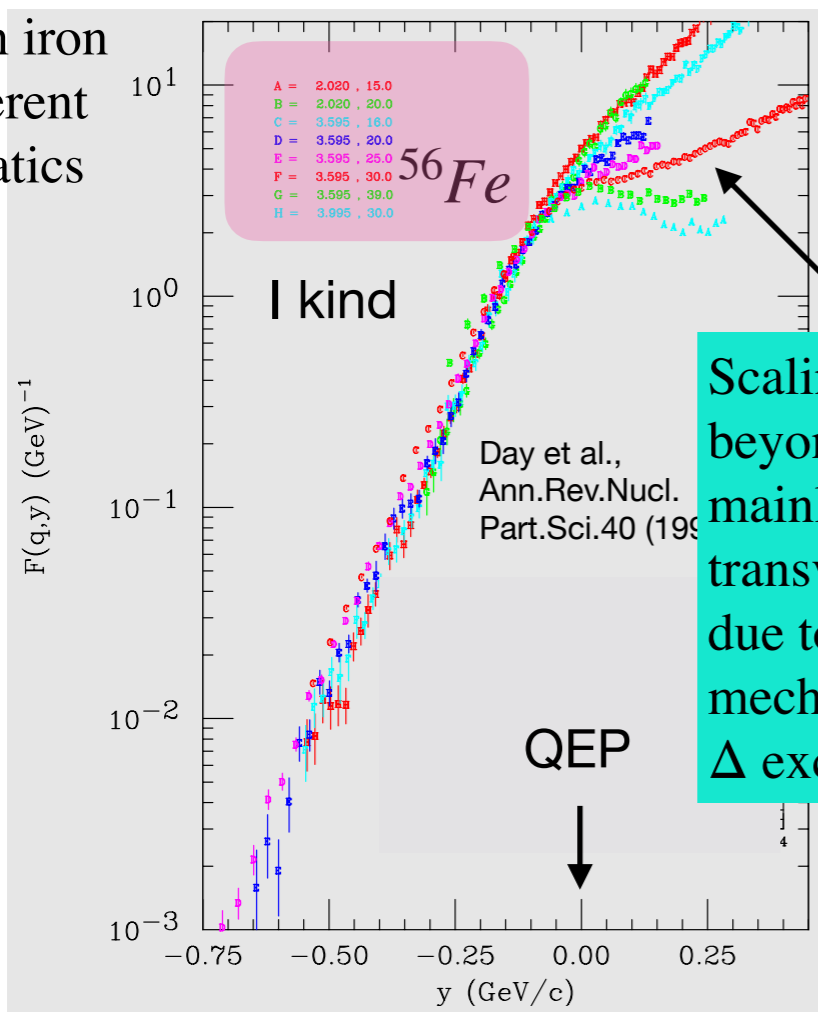
**SuperScaling function**

$$f(q, \omega; k_F) = k_F \times \frac{[d^2\sigma/d\omega d\Omega_e]_{exp} \quad q \gtrsim 300 \text{ MeV}/c}{\bar{\sigma}_{eN}(q, \omega; p = p_{min}, \mathcal{E} = 0)} \longrightarrow f(\psi)$$

embodies nuclear effects

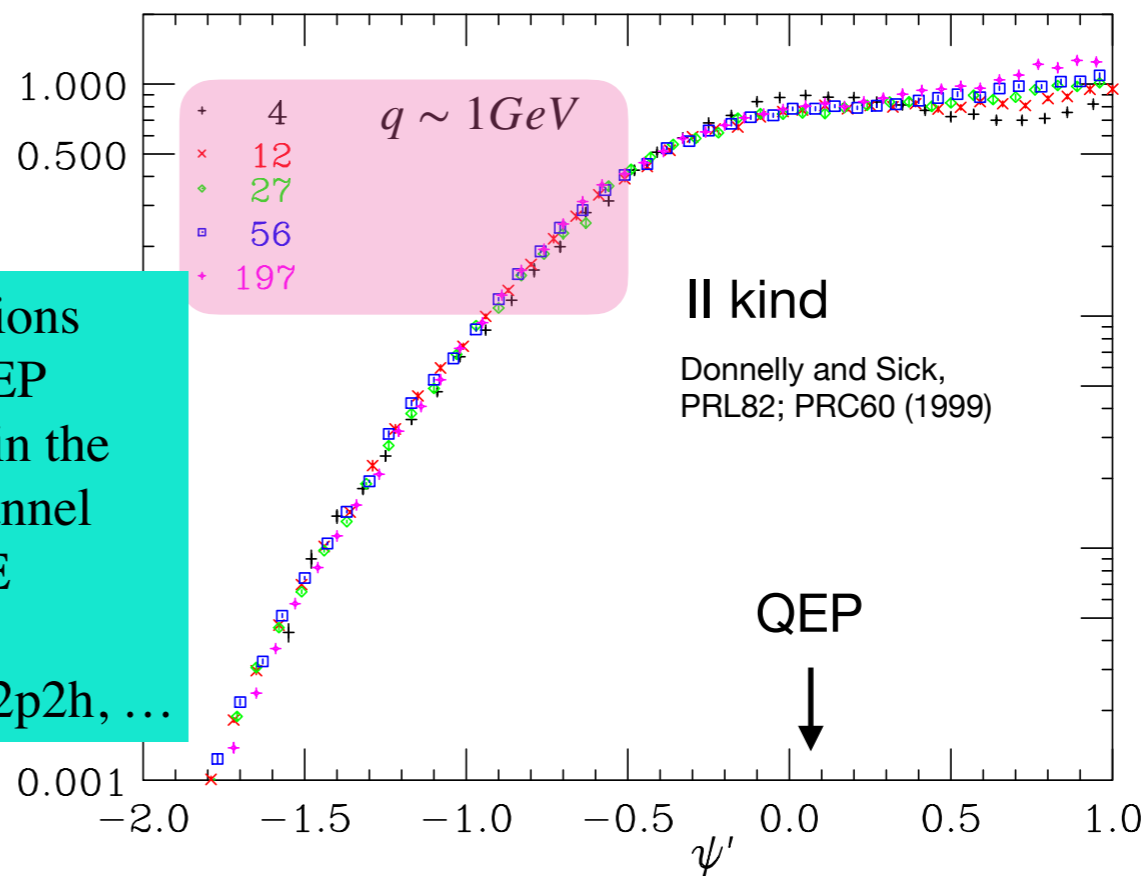
**Scaling variable**  $\psi \equiv \psi(q, \omega)$  - or  $y(q, \omega)$  - is a specific combination of the two variables  $q$  and  $\omega$  (analogous to  $x$  in DIS)

data on iron at different kinematics



Scaling violations beyond the QEP mainly occur in the transverse channel due to non-QE mechanisms:  $\Delta$  excitation, 2p2h, ...

data on different nuclei at fixed kinematics



**Scaling of first kind:**

$$f(q, \omega; k_F) \rightarrow f(\psi; k_F)$$

**no dependence on kinematics**

**for a specific nucleus**

**Scaling of second kind:  $f(\psi; k_F) \rightarrow f(\psi)$**

**no dependence on the nuclear species**

**at fixed kinematics**

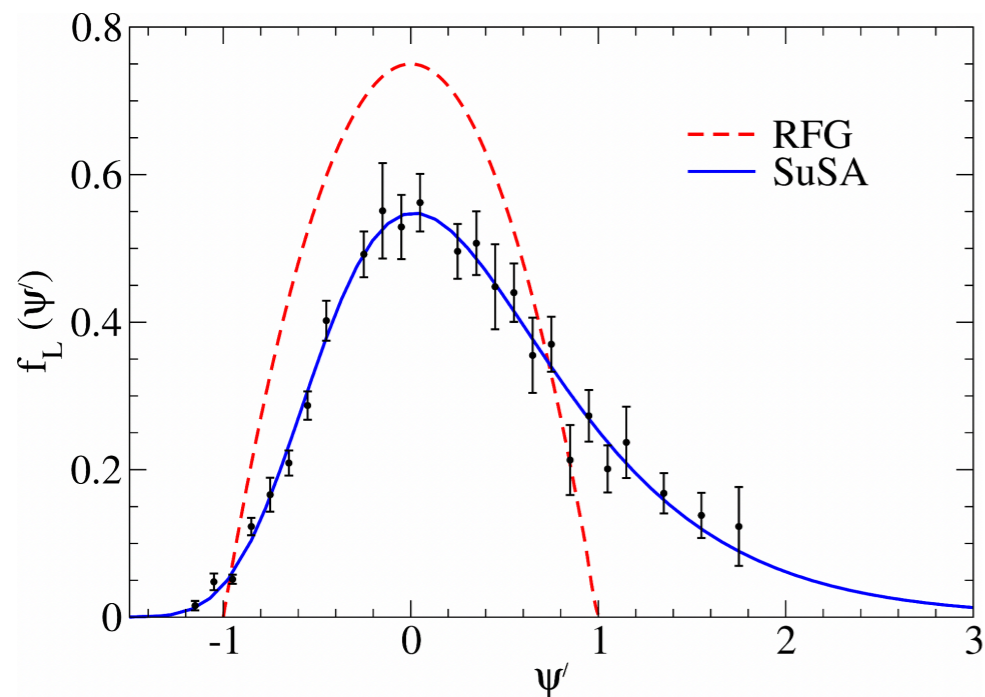
**I+II kind = SuperScaling**

# The “SuSA” and “SuSAv2” Models

## “SuSA” model (phenomenological)

[Amaro *et al.*, PRC71 (2007)]

Use the superscaling function extracted from the  $(e, e')$  world data analysis and plug it into  $(\nu_l, l^-), (\bar{\nu}_l, l^+)$



Assumption: the function  $f(\psi)$  is the same for all reaction channels (longitudinal, transverse, isoscalar, isovector...)

$$R^K(q, \omega) = k_F \times G^K(q, \omega) \times f(\psi')$$

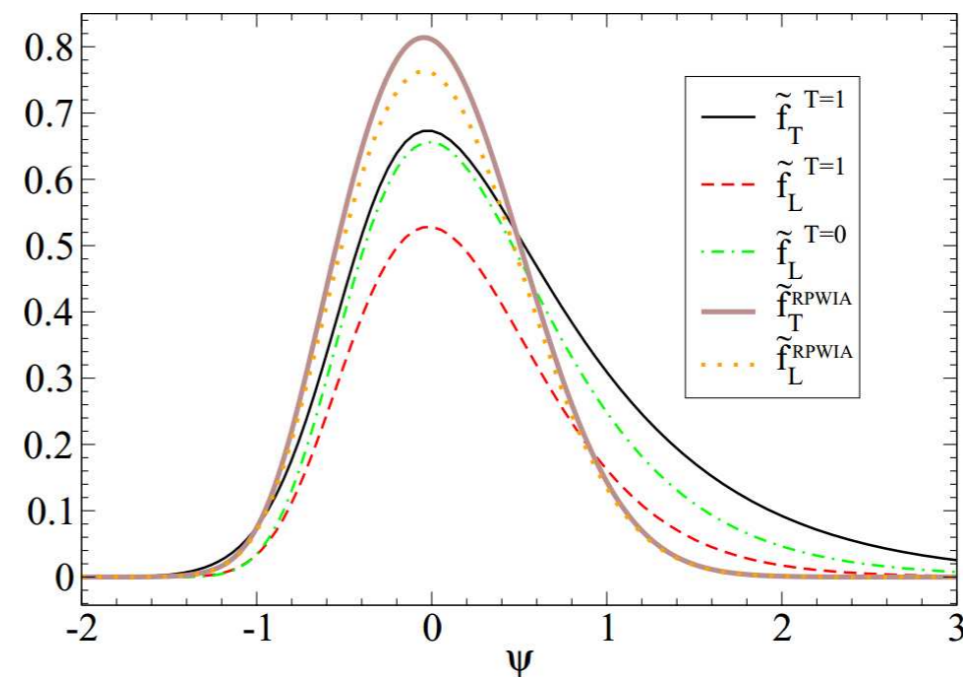
$R^K$  nuclear responses

$G^K$  single-nucleon functions

## “SuSAv2” model (microscopic)

[Gonzalez *et al.*, PRC90(2014), Megias *et al.*, PRD94 (2016)]

A set of scaling functions  $\tilde{f}^K$  is calculated in the **Relativistic Mean Field** model for all reaction channels (L/T, isovector/isoscalar, V/A)



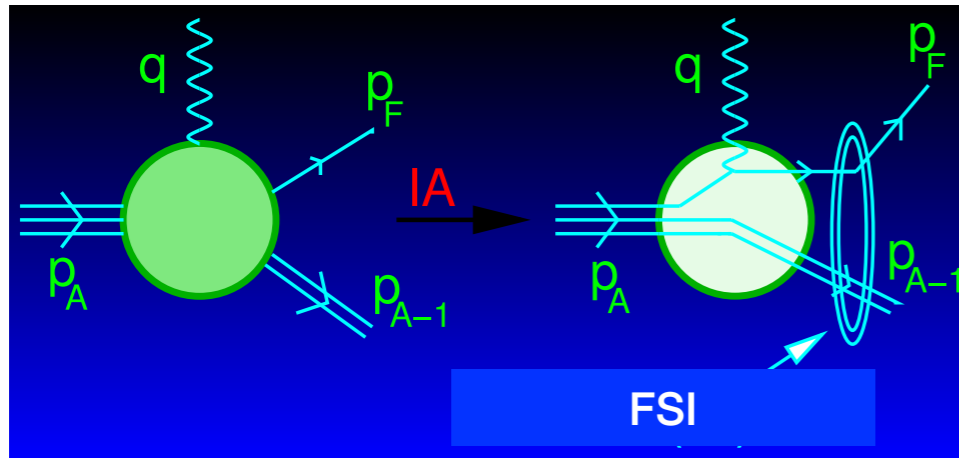
The shortcoming of the RMF of being too strong at high energies is corrected for by introducing a q-dependent blending functions which **mixes RMF and RPWIA final states**. This introduces few parameters, which are fitted once and for all to Carbon  $(e, e')$  data.

Equivalently, one can introduce energy-dependent S and V potentials [Gonzalez *et al.*, PRC101 (2020)].

# The Relativistic Mean Field Model

The RMF model is based on the **impulse approximation**:

scattering off a nucleus = incoherent sum of single nucleon scattering processes



The nucleon wave functions are finite nucleus solutions of the Dirac equation with phenomenological relativistic scalar and vector potentials obtained from a Walecka-type Lagrangian fitted to properties of nuclear radii and masses:

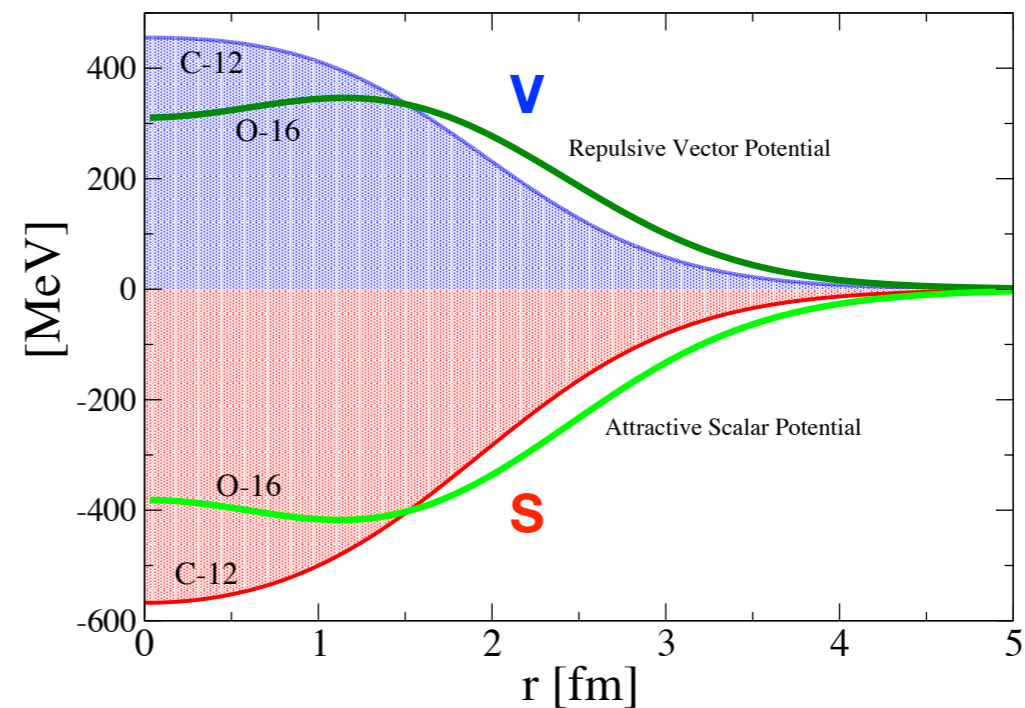
$$(i\gamma^\mu \partial_\mu - M - S + V) \psi(\vec{r}, t) = 0$$

**Nuclear Current**  $\Rightarrow$  **One-body operator**

$$J_N^\mu(\omega, \vec{q}) = \int d\vec{p} \bar{\Psi}_F(\vec{p} + \vec{q}) \hat{J}_N^\mu \Psi_B(\vec{p})$$

**Bound wave function**

$$\Psi_B = \begin{pmatrix} \phi^{up} \\ \phi^{down} \end{pmatrix} = \begin{pmatrix} \phi^{up} \\ \frac{\sigma \cdot \mathbf{p}}{E + M + S - V} \phi^{up} \end{pmatrix} = \alpha u + \beta v$$

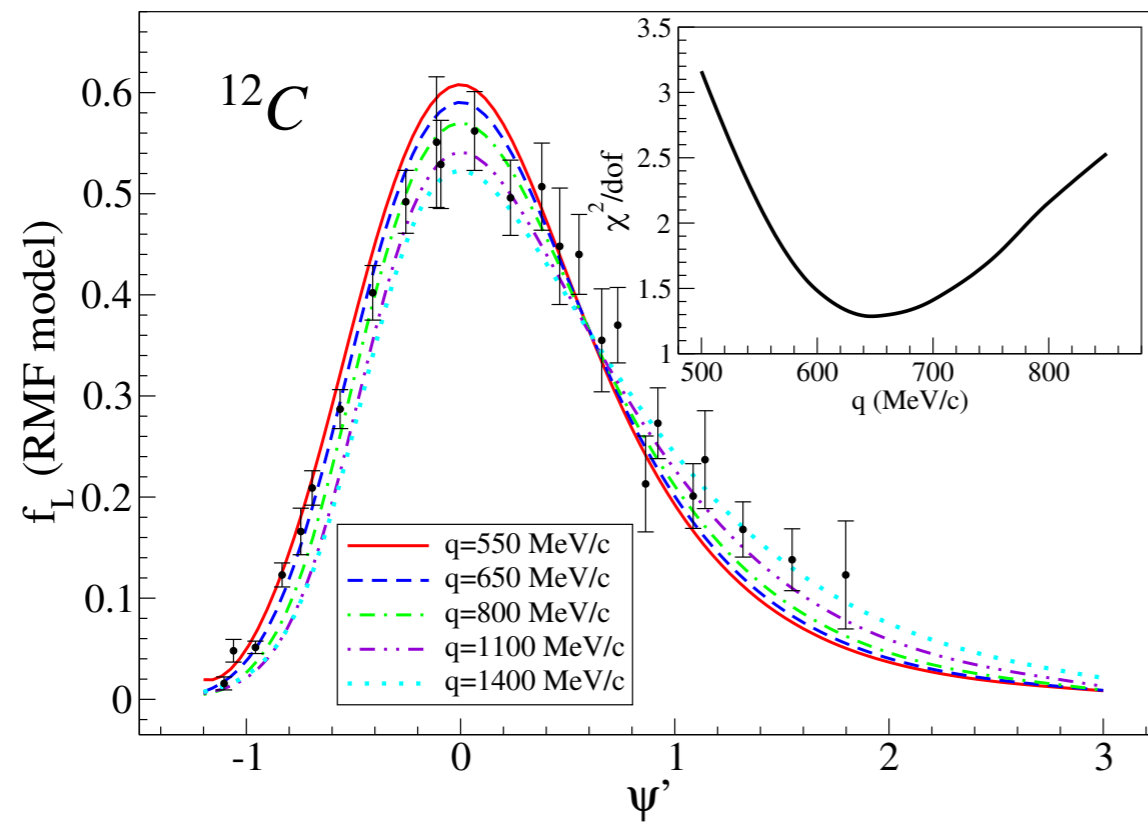


**Ejected nucleon wave function** is distorted by final-state interactions (FSI).

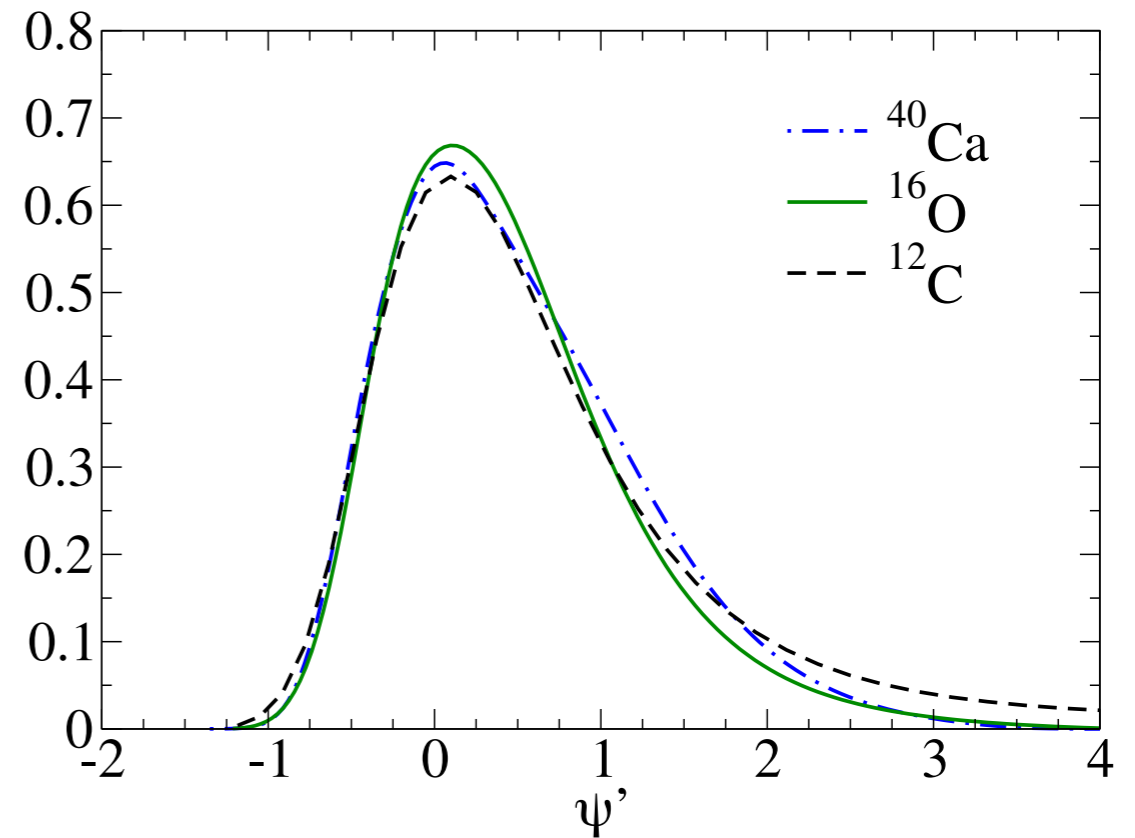
In the RMF model it is a scattering solution of the same Dirac equation used to describe the bound state. Orthogonality is preserved: the initial and final nucleon wave functions are eigenstates of the same H

# Relativistic Mean Field Model: superscaling test

## I kind scaling

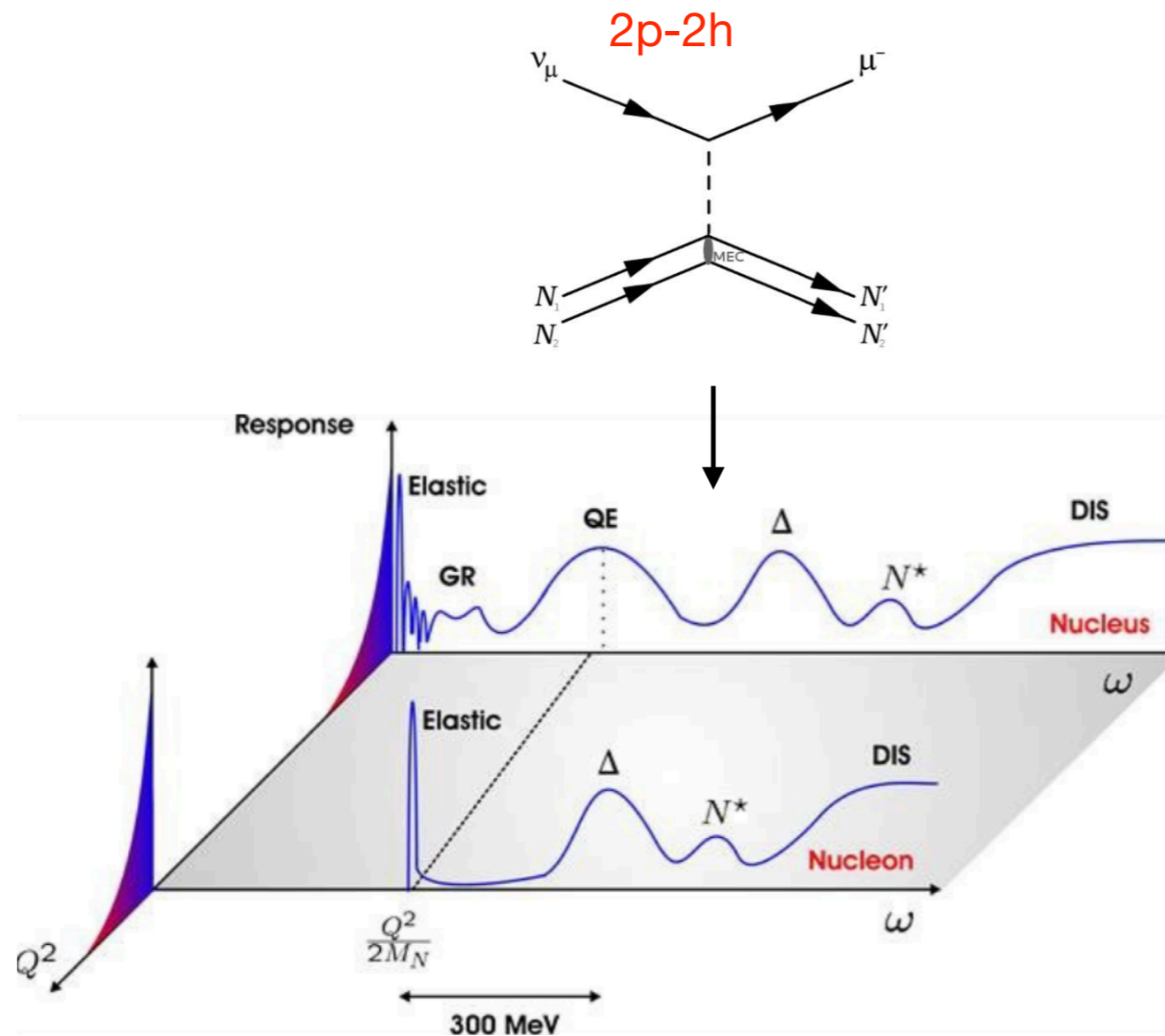


## II kind scaling



Violations of I and II kind scaling are compatible with data

# Beyond the Impulse Approximation: Meson Exchange Currents and 2p2h excitations



The probe interacts with a correlated pair of nucleons: beyond IA

Martini *et al.*, *Phys.Rev.C* 80 (2009) 065501

first showed that this process contributes significantly to neutrino cross sections in oscillation experiments, solving the MiniBooNE “axial mass puzzle”

# Meson Exchange Currents

De Pace et al., Nucl.Phys. A726 (2003) 303-326  
 Ruiz Simo et al., J.Phys. G44 (2017) no.6, 065105

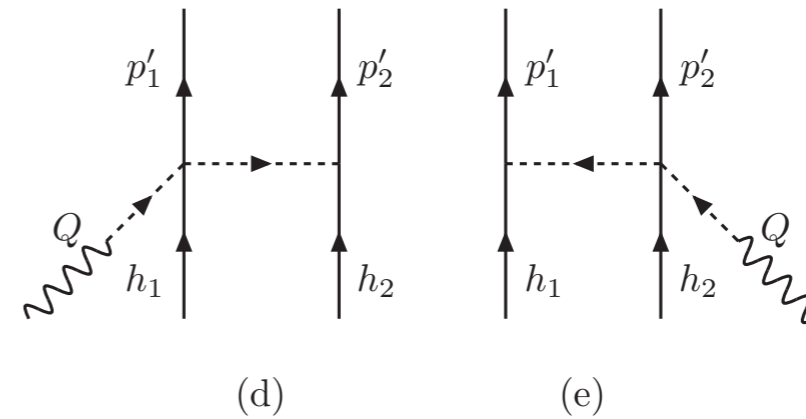
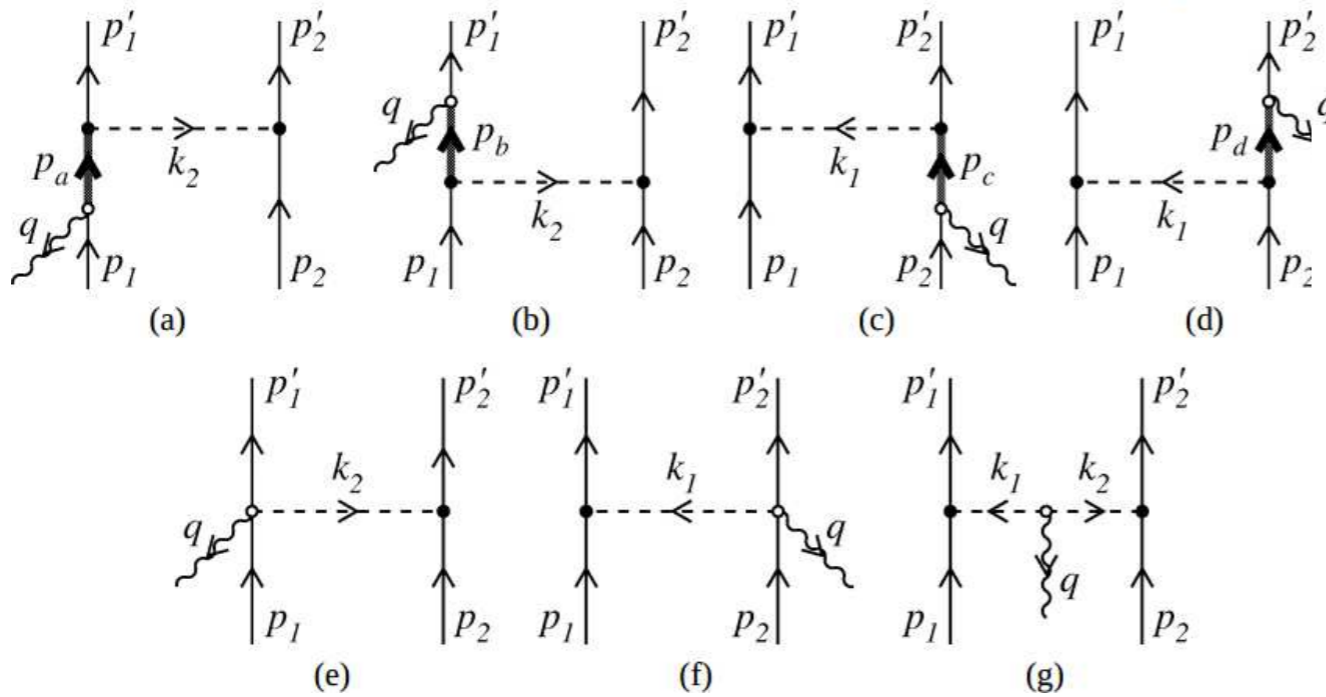
electromagnetic MEC  
 extension to weak sector

## Two-body currents in free space

“ $\Delta$  pole”

“Pion pole”

(only for neutrinos, purely axial)



“Seagull” or “contact”

“Pion in flight”



# 2p2h MEC many-body diagrams

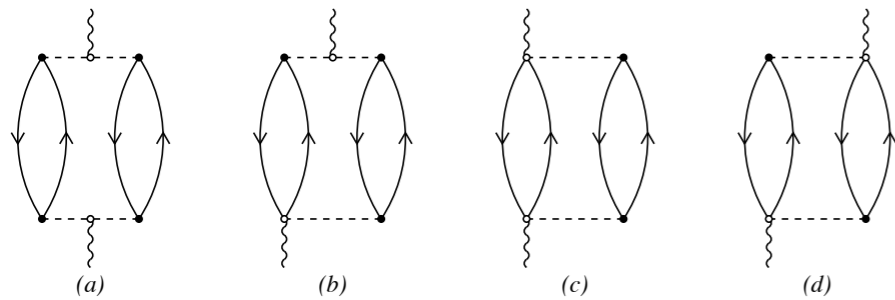


FIG. 2: The direct pionic contributions to the MEC 2p-2h response function.

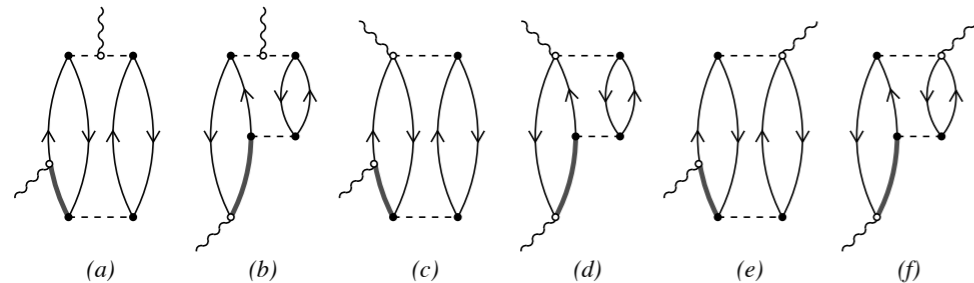


FIG. 3: The direct pionic/ $\Delta$  interference contributions to the MEC 2p-2h response function.

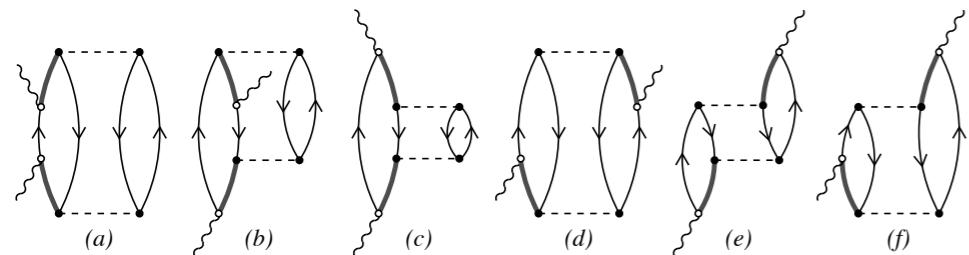


FIG. 4: The direct  $\Delta$  contributions to the MEC 2p-2h response function.

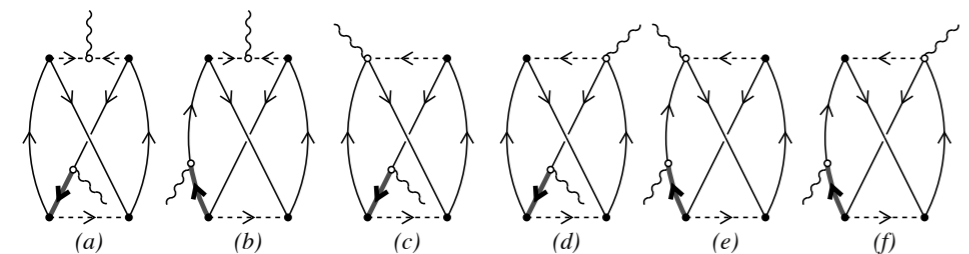


FIG. 5: The exchange pionic/ $\Delta$  interference contributions to the MEC 2p-2h response function.

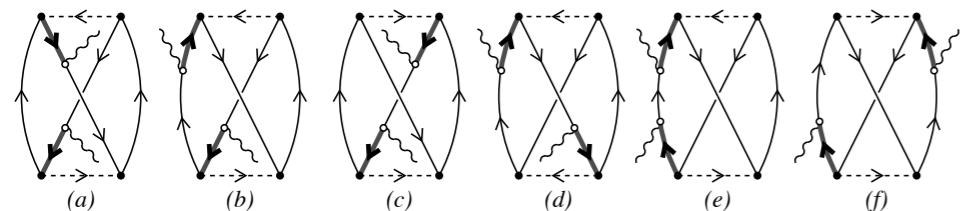


FIG. 6: The exchange  $\Delta$  contributions to the MEC 2p-2h response function.

**In the medium**, huge amount of many-body diagrams, corresponding to the excitation of **2p2h** states.

In the RFG the corresponding hadronic tensor is:

$$W_{2p-2h}^{\mu\nu} = \frac{V}{(2\pi)^9} \int d^3 p'_1 d^3 p'_2 d^3 h_1 d^3 h_2 \frac{m_N^4}{E_1 E_2 E'_1 E'_2} \times r^{\mu\nu}(\mathbf{p}'_1, \mathbf{p}'_2, \mathbf{h}_1, \mathbf{h}_2) \delta(E'_1 + E'_2 - E_1 - E_2 - \omega) \times \Theta(p'_1, p'_2, h_1, h_2) \delta(\mathbf{p}'_1 + \mathbf{p}'_2 - \mathbf{h}_1 - \mathbf{h}_2 - \mathbf{q}),$$

$$\Theta(p'_1, p'_2, h_1, h_2) = \theta(p'_2 - k_F) \theta(p'_1 - k_F) \theta(k_F - h_1) \theta(k_F - h_2).$$

$$r^{\mu\nu}(\mathbf{p}'_1, \mathbf{p}'_2, \mathbf{h}_1, \mathbf{h}_2) = \frac{1}{4} \sum_{s,t} j^\mu(1', 2', 1, 2)_A^* j^\nu(1', 2', 1, 2)_A,$$

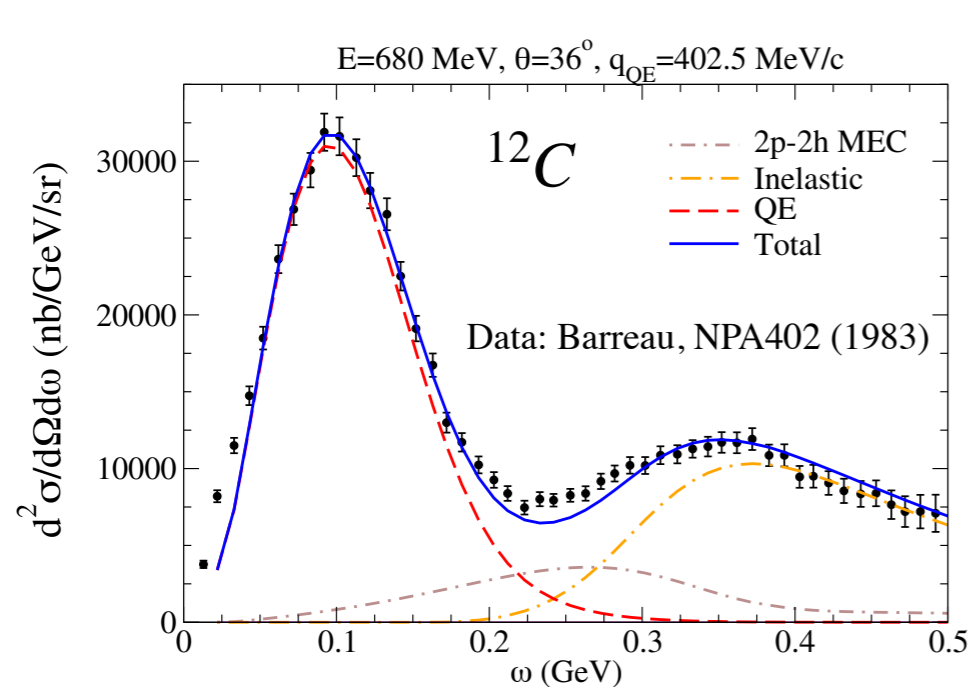
- fully relativistic calculation based on RFG
- all many-body diagrams involving 2 pions included
- each diagram is a 7D integral+flux integration
- np, nn and pp can be separated
- numerical results have been parametrised as functions of  $(q, \omega)$  for use in MC generators

## Results:

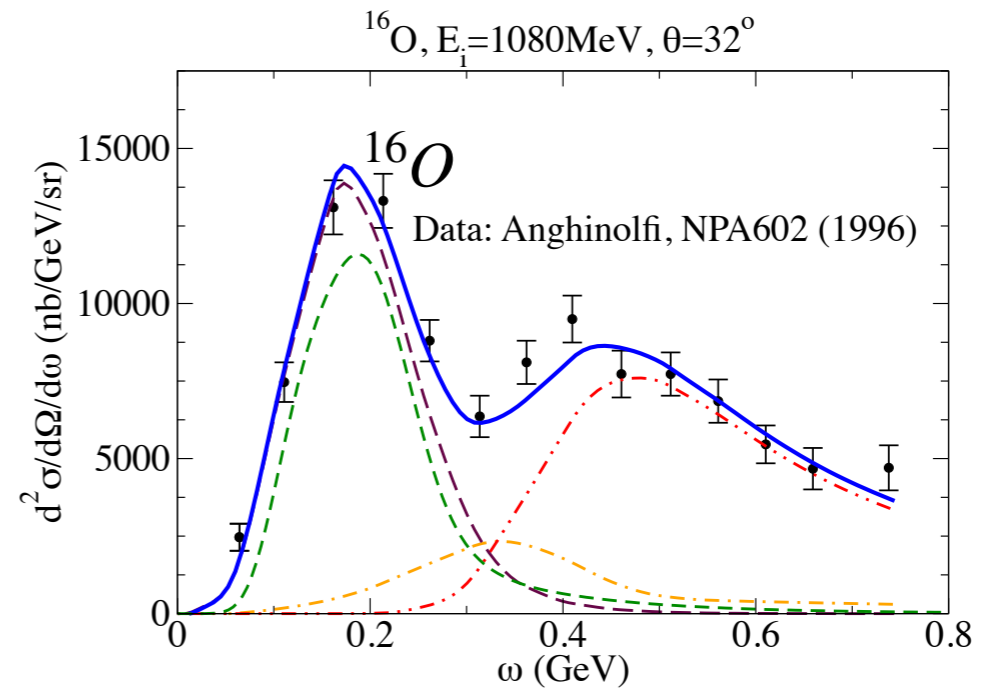
application of SuSAv2 (RMF+2p2h) model

1.  $A(e, e')X$  validation: inclusive electron scattering
2.  $A(\nu_\mu, \mu)X$  charged current neutrino scattering  
“CCQE-like” or “CC0 $\pi$ ”  
no pions in the final state
3.  $A(\nu_\mu, \mu p)X$  semi-inclusive neutrino scattering

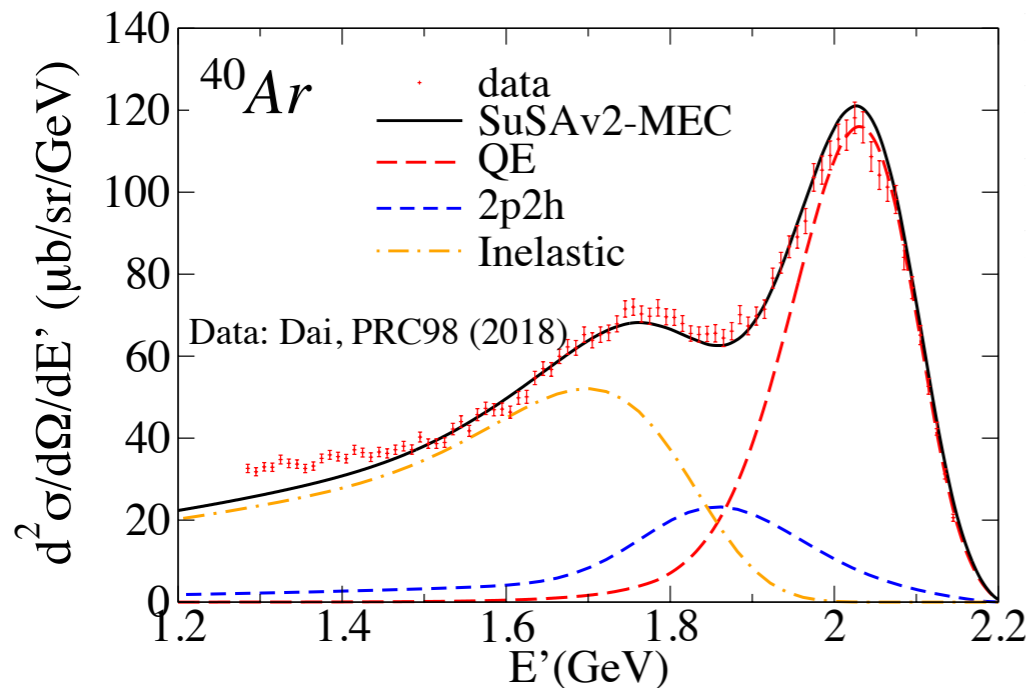
# Validation of the SuSAv2 model : (e,e') on C, O and Ar



G.D. Megias *et al.*, PRD94 (2016)



G.D. Megias *et al.*, JPG46 (2019)

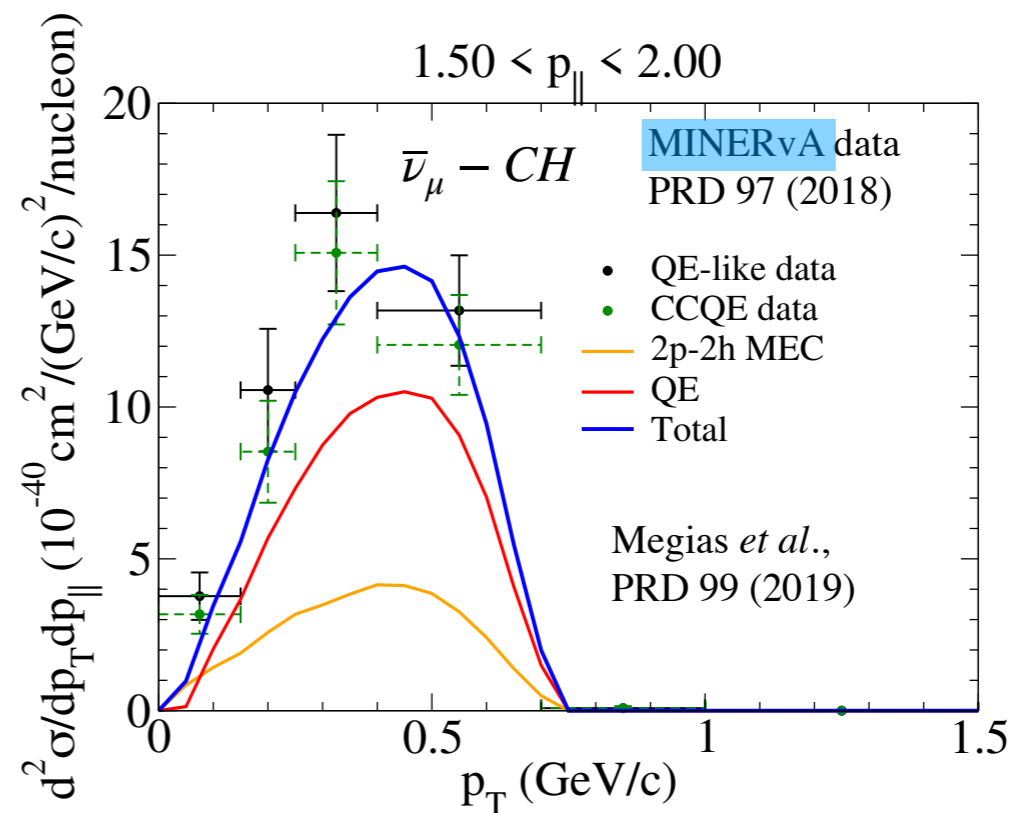
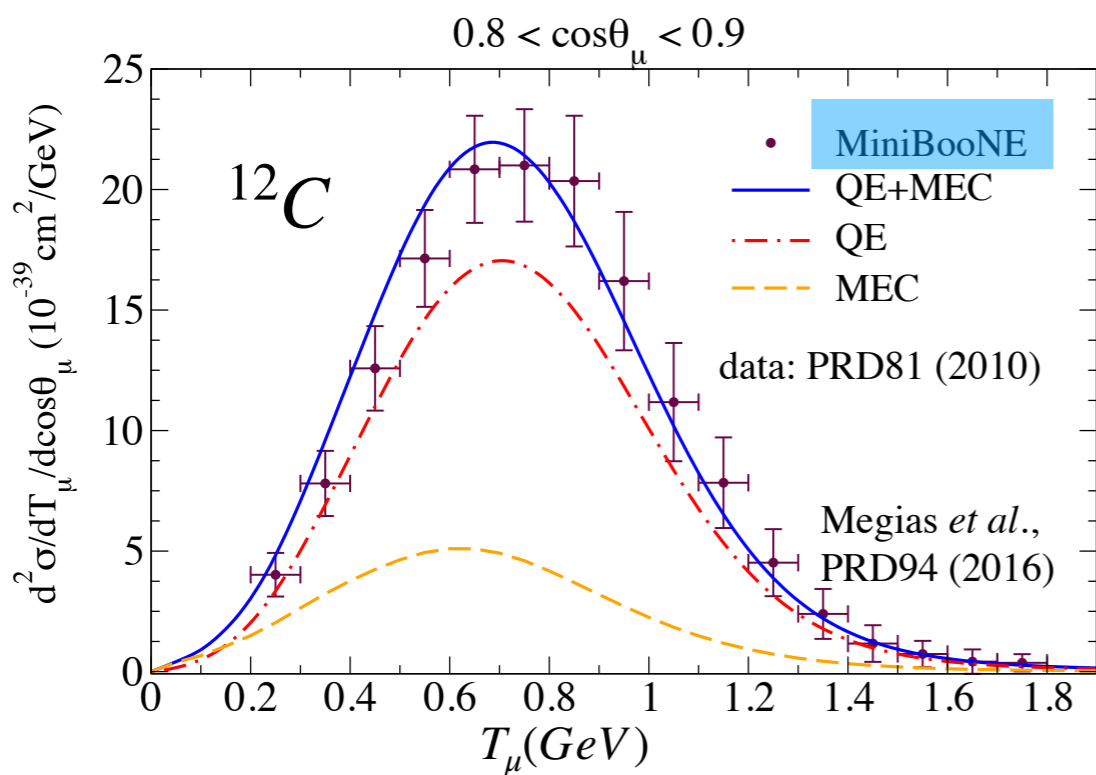
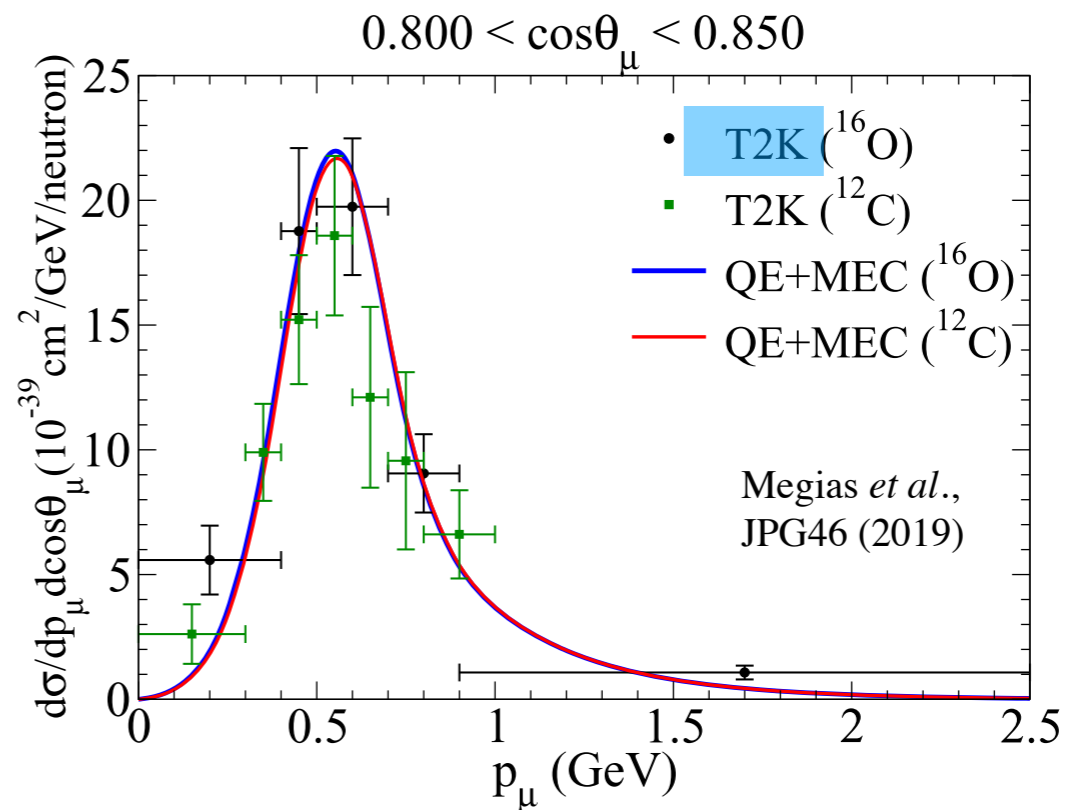
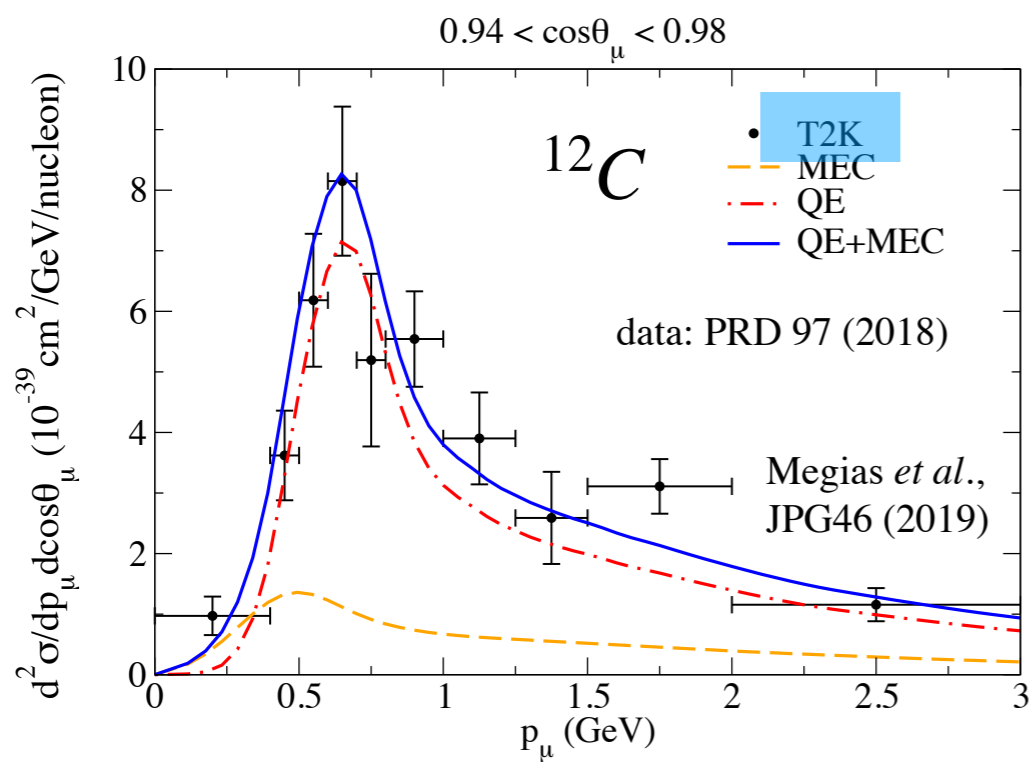


MBB *et al.*, PRC99 (2019)

Good agreement with data for different nuclei in a wide kinematical region, with the exception of the very low  $q$  regime, where the superscaling approach and IA fail.

The inelastic region is modelled using the Bosted and Christy parametrization of inelastic structure functions  $w_1, w_2$  and a generalisation of the scaling variable to a generic excitation:  $\psi(m_N) \rightarrow \psi(m_N^*)$

# $(\nu_\mu, \mu^-)$ CC0 $\pi$ cross section



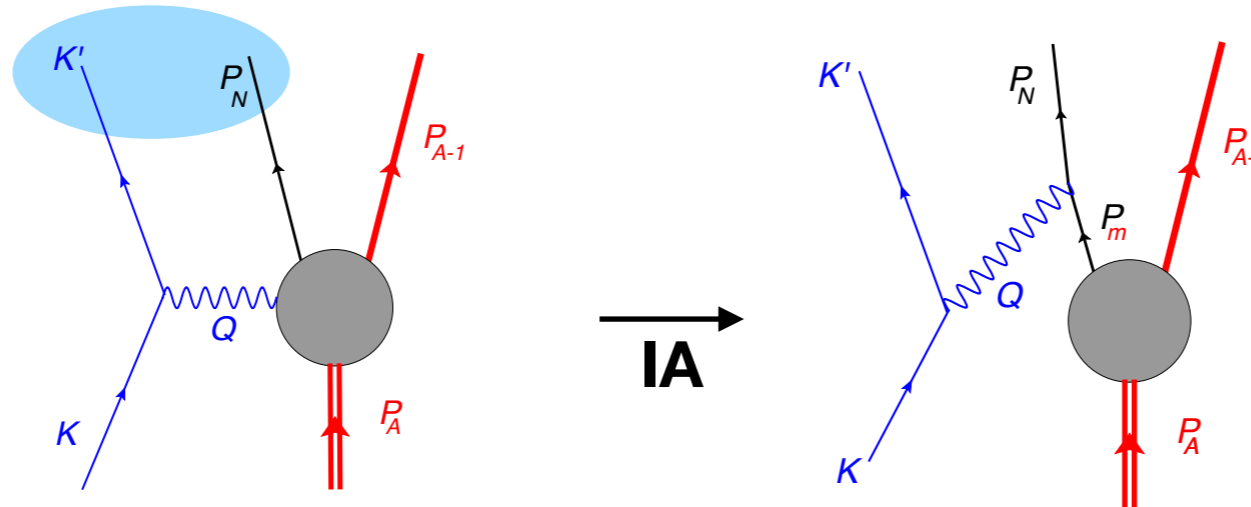
Semi-inclusive observables, where one final nucleon is observed in coincidence with the outgoing lepton, are more sensitive to the details of the nuclear structure and can better constrain the extraction of the neutrino energy

$$E_m = \omega - T_N \simeq \mathcal{E} + E_s$$

missing energy

$$\vec{p}_m = \vec{q} - \vec{p}_N$$

missing momentum



$$\left\langle \frac{d\sigma}{dk' d\Omega_{k'} dp_N d\Omega_N^L} \right\rangle = \frac{(G_F \cos \theta_c k' p_N)^2 m_N}{8\varepsilon' E_N (2\pi)^6} \int_0^\infty dk \frac{P(k)}{k} v_0 \mathcal{F}_\chi^2 S(p_m, E_m(\mathcal{E}, p_m)) \theta(\mathcal{E})$$

**nuclear spectral function**

**elementary cross section  
(10 response functions)**

$$S(p, E) = \langle \psi_0 | a^\dagger(p) \delta[\hat{H} - (E_0 - E)] a(p) | \psi_0 \rangle$$

joint probability of finding a nucleon of given momentum  $p$  in the nuclear ground state  $A$  and reaching final states in the daughter nucleus  $A-1$  characterised by missing energy  $E$

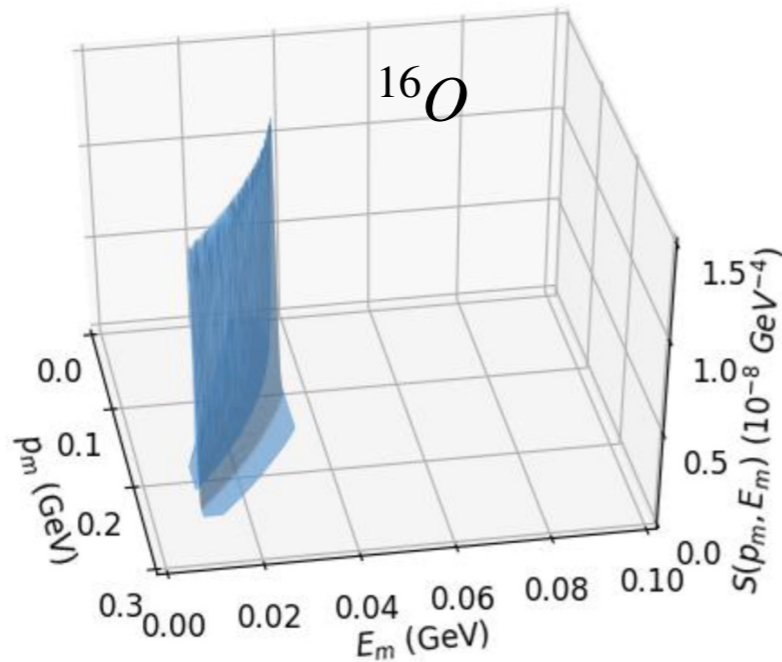
$$\begin{aligned} \mathcal{F}_\chi^2 &= \frac{2}{v_0} L_{\mu\nu} W^{\mu\nu} \\ &= V_{CC}(R_{VV}^{CC} + R_{AA}^{CC}) + 2V_{CL}(R_{VV}^{CL} + R_{AA}^{CL}) \\ &\quad + V_{LL}(R_{VV}^{LL} + R_{AA}^{LL}) + V_T(R_{VV}^T + R_{AA}^T) \\ &\quad + V_{TT}(R_{VV}^{TT} + R_{AA}^{TT}) + V_{TC}(R_{VV}^{TC} + R_{AA}^{TC}) \\ &\quad + V_{TL}(R_{VV}^{TL} + R_{AA}^{TL}) \\ &\quad - \chi \left( V_{T'} R_{VA}^{T'} + V_{TC'} R_{VA}^{TC'} + V_{TL'} R_{VA}^{TL'} \right). \end{aligned}$$

5 new responses which vanish after integrating over the final nucleon

# Spectral function models

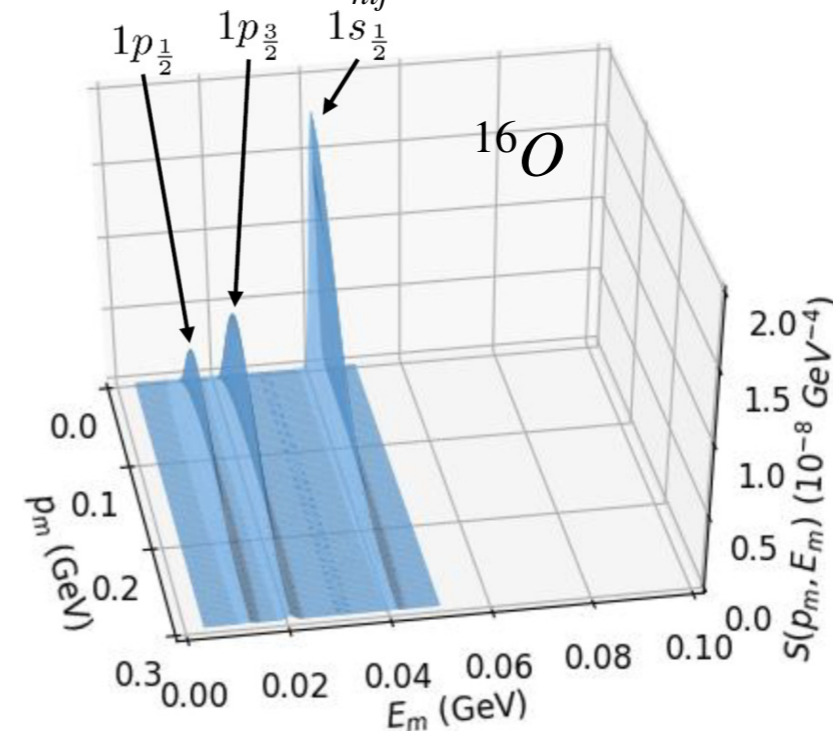
## RFG

$$S_{RFG}(p, E) = \theta(p_F - p) \delta\left(E - \sqrt{p^2 + m_N^2}\right)$$

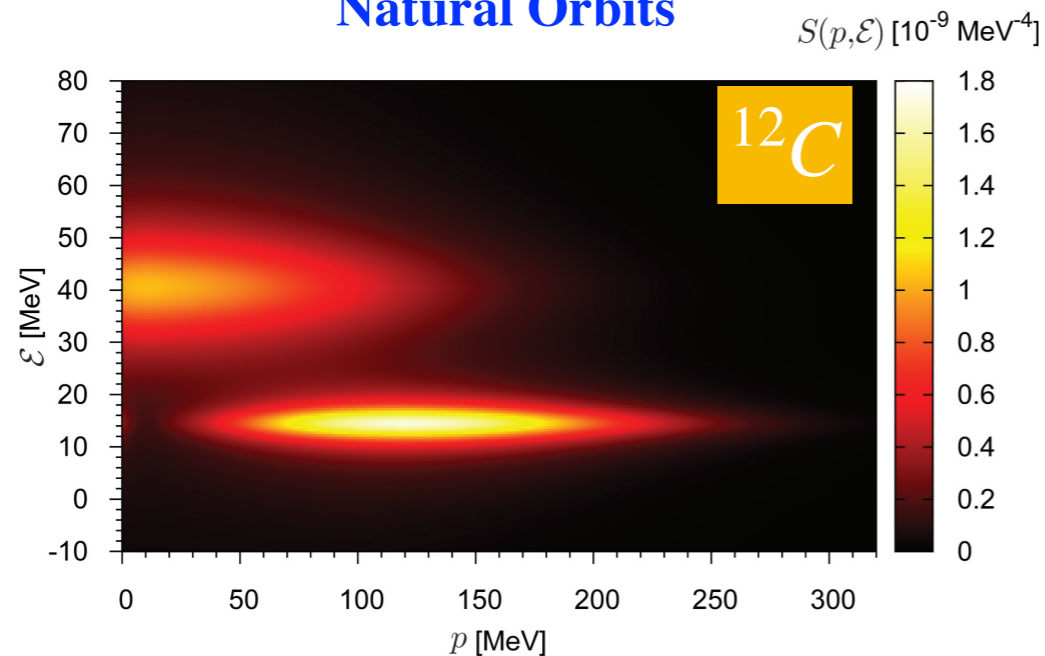


## IPSM/RMF

$$S_{IPSM}(p, E) = \sum_{nlj} (2j + 1) n_{nlj}(p) \delta(E - E_{nlj})$$



## Natural Orbits



$$S_{NO}(p, E) = \frac{1}{2\pi A} \sum_{\alpha} (2j_{\alpha} + 1) N_{\alpha} |\psi_{\alpha}(p)|^2 L_{\Gamma_{\alpha}}(E - E_i)$$

$0 \leq N_{\alpha} \leq 1$  natural occupation numbers

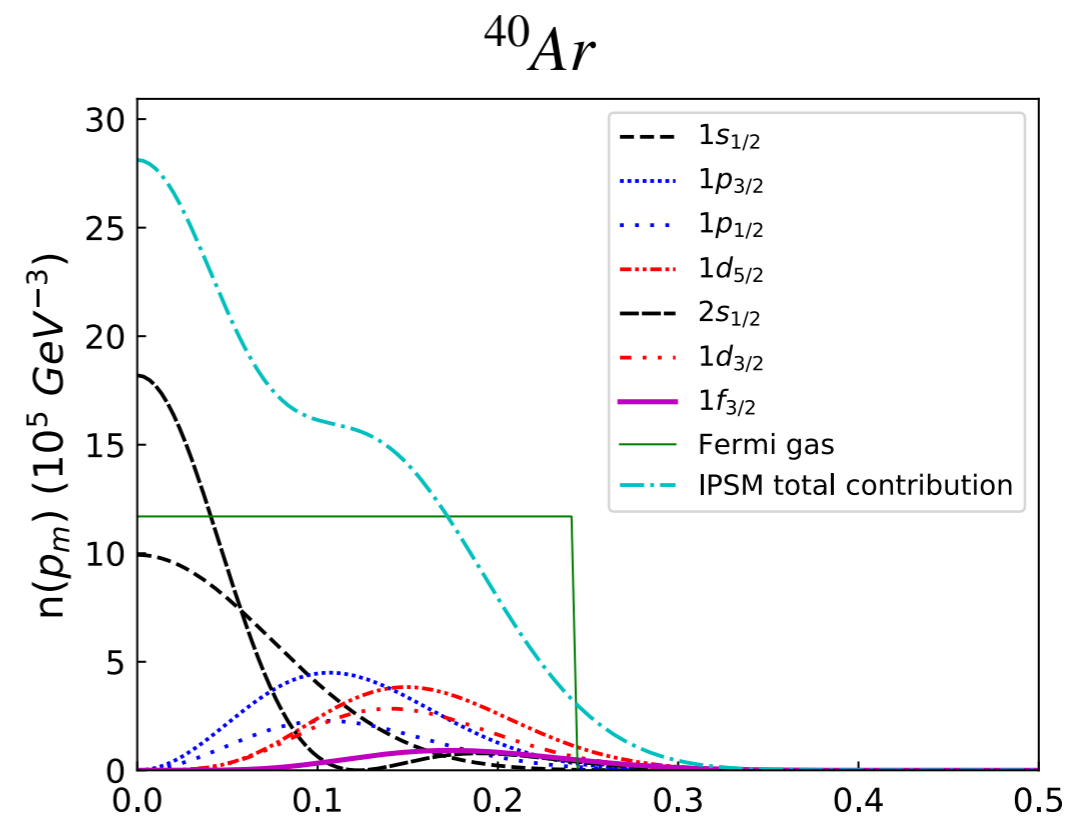
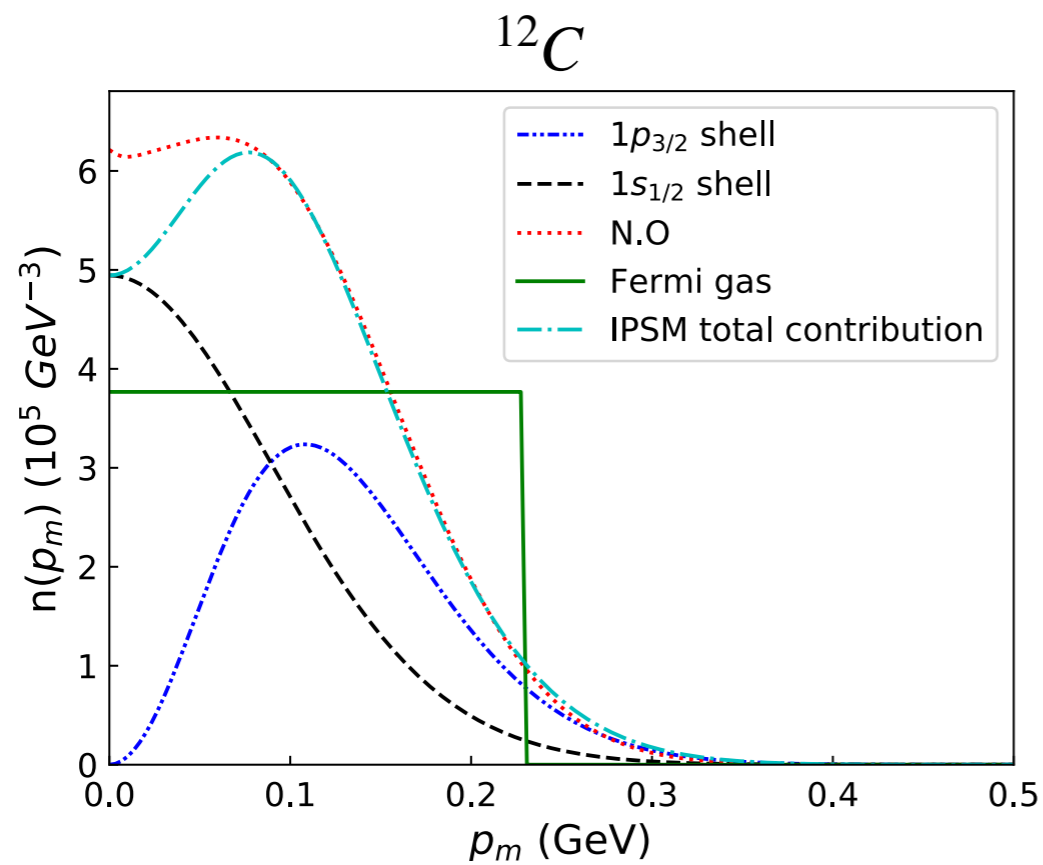
$L_{\Gamma}$  Lorentzian distribution

Natural orbitals include NN short range correlations

Ivanov *et al.*, PRC.89.014607 (2014)

# Momentum distribution

$$n(p_m) = \int_0^\infty S(p_m, E_m) dE_m$$



J.M. Franco Patino *et al.*, PRC 102, 064626 (2020)

# 6th differential semi-inclusive cross sections

$${}^{40}\text{Ar}(\nu_\mu, \mu^- p){}^{39}\text{Cl}$$

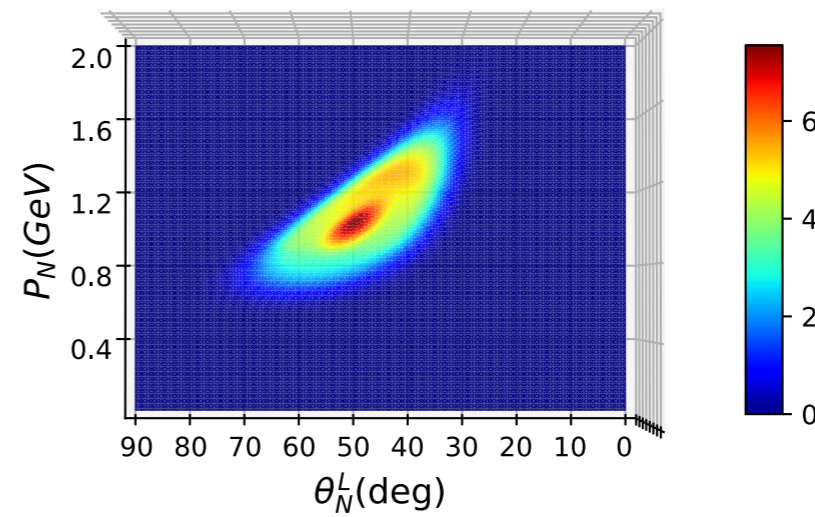
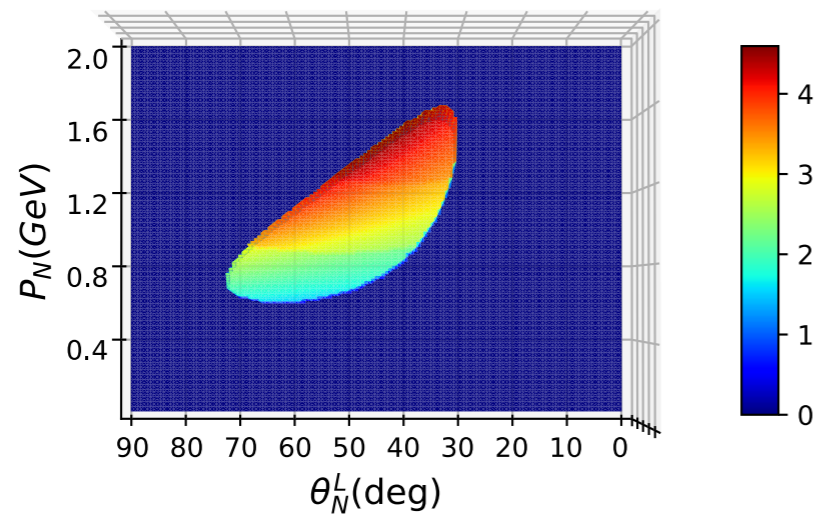
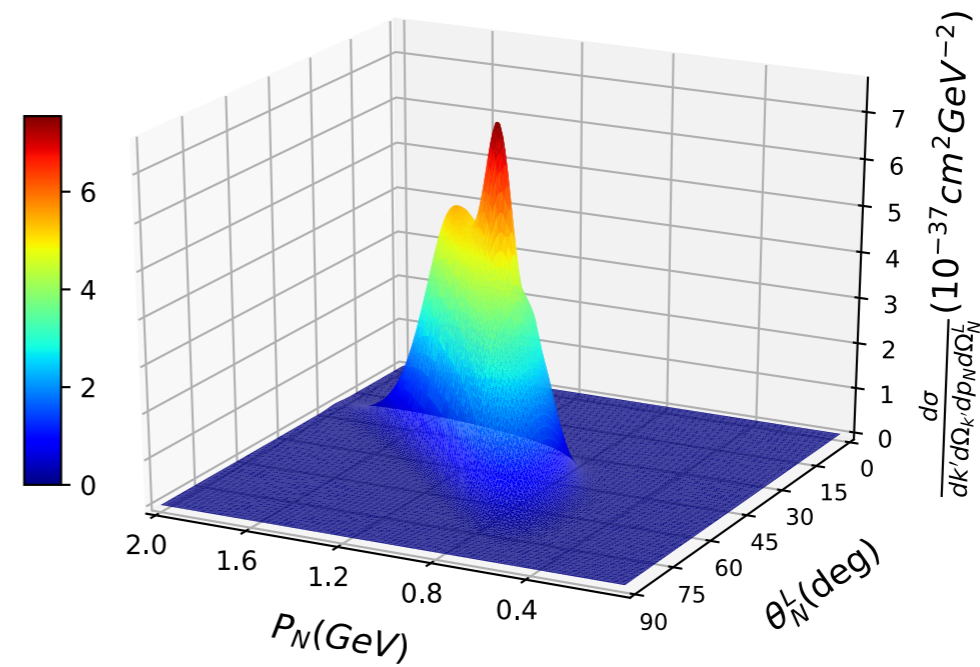
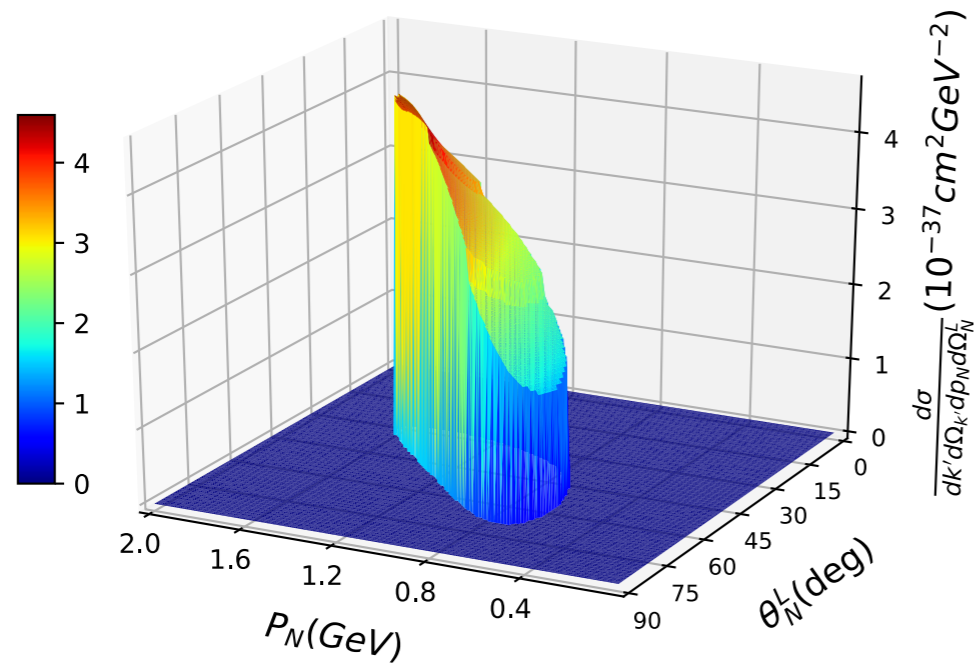
RPWIA

$$k' = 1.5\text{GeV}, \theta_\mu = 30^\circ, \phi_N^L = \pi$$

DUNE flux

RFG

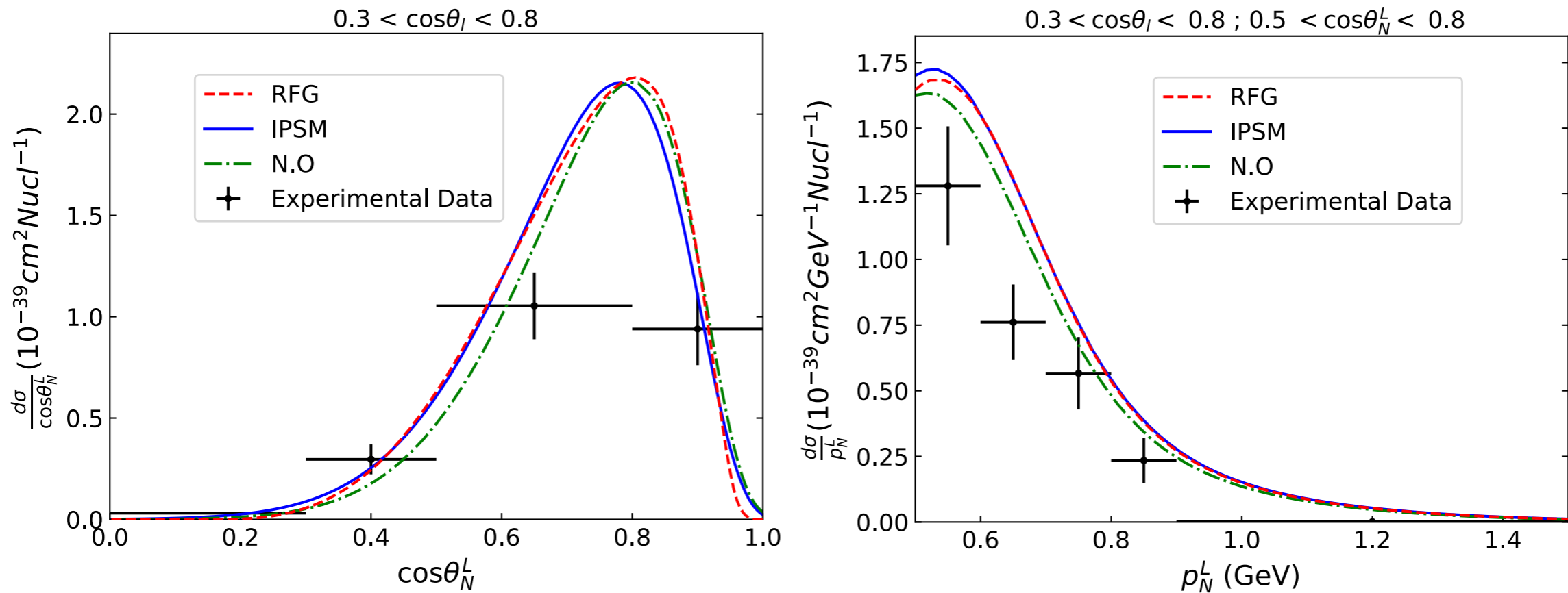
IPSM



J.M. Franco Patino *et al.*, PRC 102, 064626 (2020)



# Comparison with neutrino cross sections versus proton kinematics



J.M. Franco Patino *et al.*, PRC 102, 064626 (2020)

Data from K. Abe *et al.* (The T2K Collaboration), PRD 98, 032003 (2018)

Tiny differences between RFG and IPSM.

Natural Orbit (SRC) predicts lower cross sections.

**Warning: RPWIA**

Final State Interactions and 2p2h not yet included (work in progress)

# Single Transverse Variables

Single transverse kinematic unbalance

$$\delta\vec{p}_T \equiv \vec{p}_T^{\ell'} + \vec{p}_T^{N'}$$

$$\delta\alpha_T \equiv \arccos \frac{-\vec{p}_T^{\ell'} \cdot \delta\vec{p}_T}{p_T^{\ell'} \delta p_T}$$

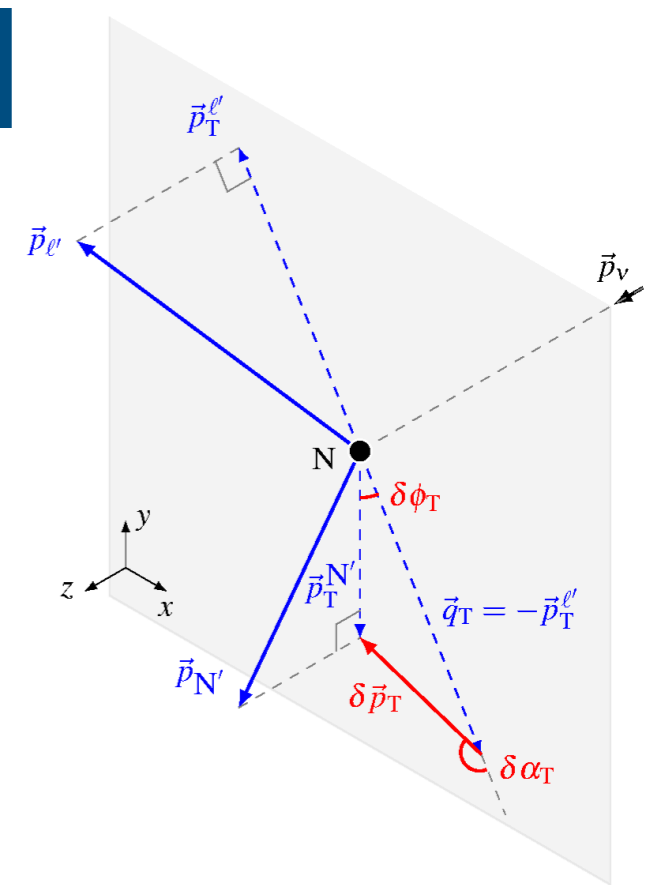
$$\delta\phi_T \equiv \arccos \frac{-\vec{p}_T^{\ell'} \cdot \vec{p}_T^{N'}}{p_T^{\ell'} p_T^{N'}}$$

Lu et al., PRC94, 015503 (2016)

On a free nucleon  $\vec{p}_T^{\ell'} = -\vec{p}_T^{N'}$ :

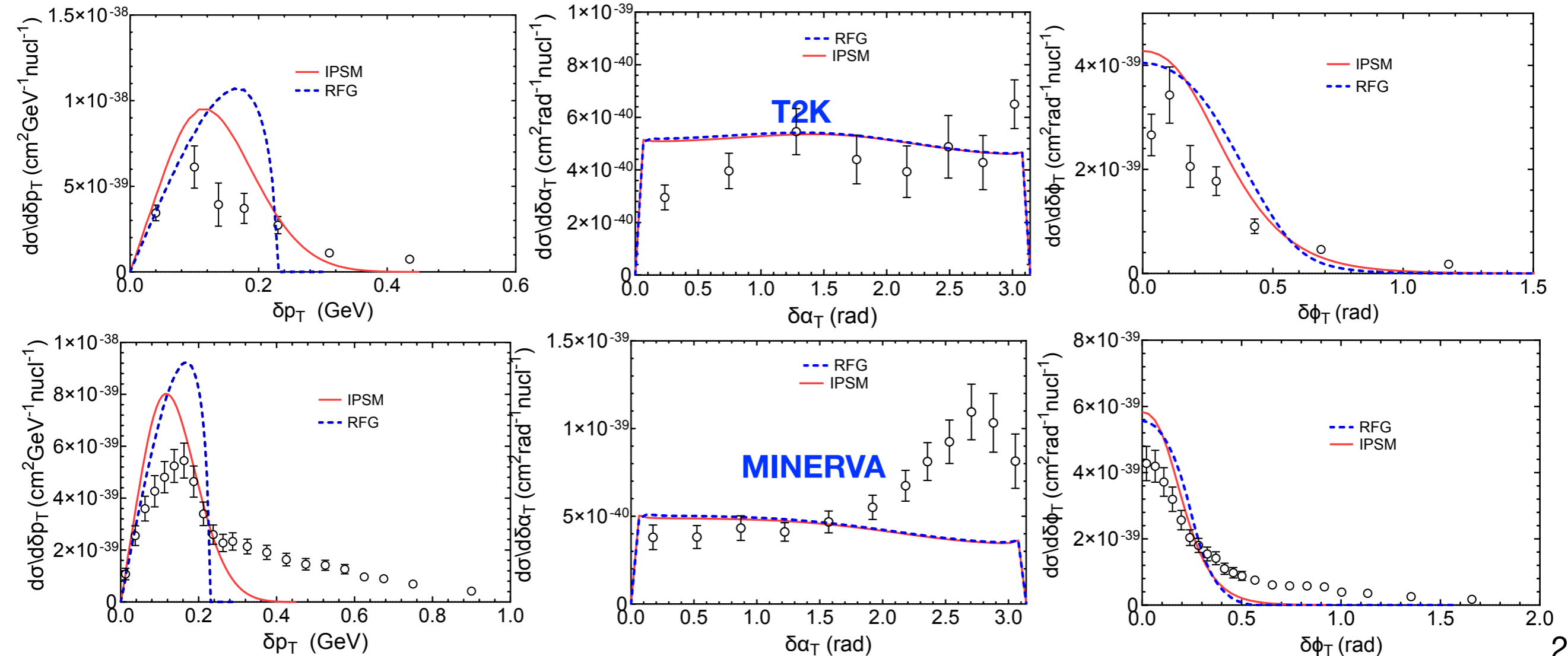
$$\delta p_T = \delta\phi_T = 0$$

$\delta\alpha_T$  undefined



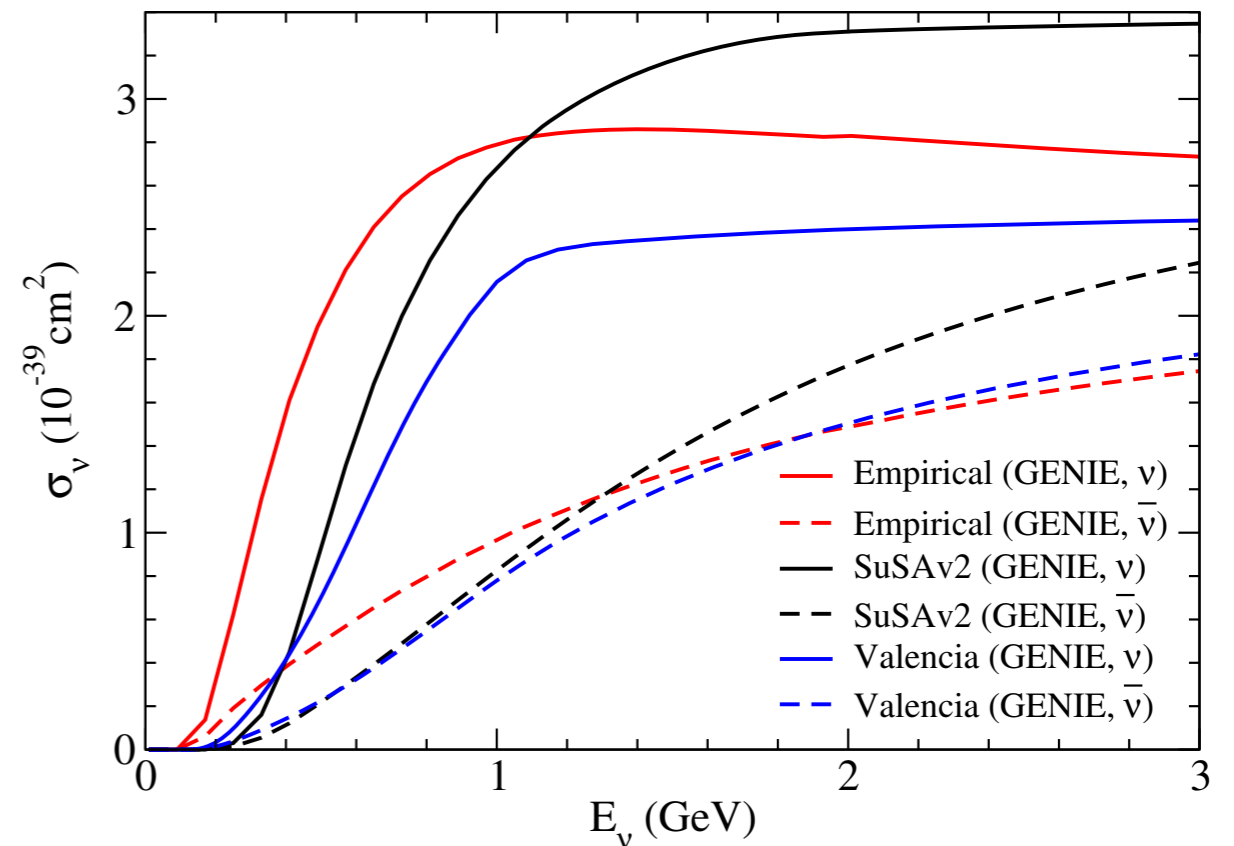
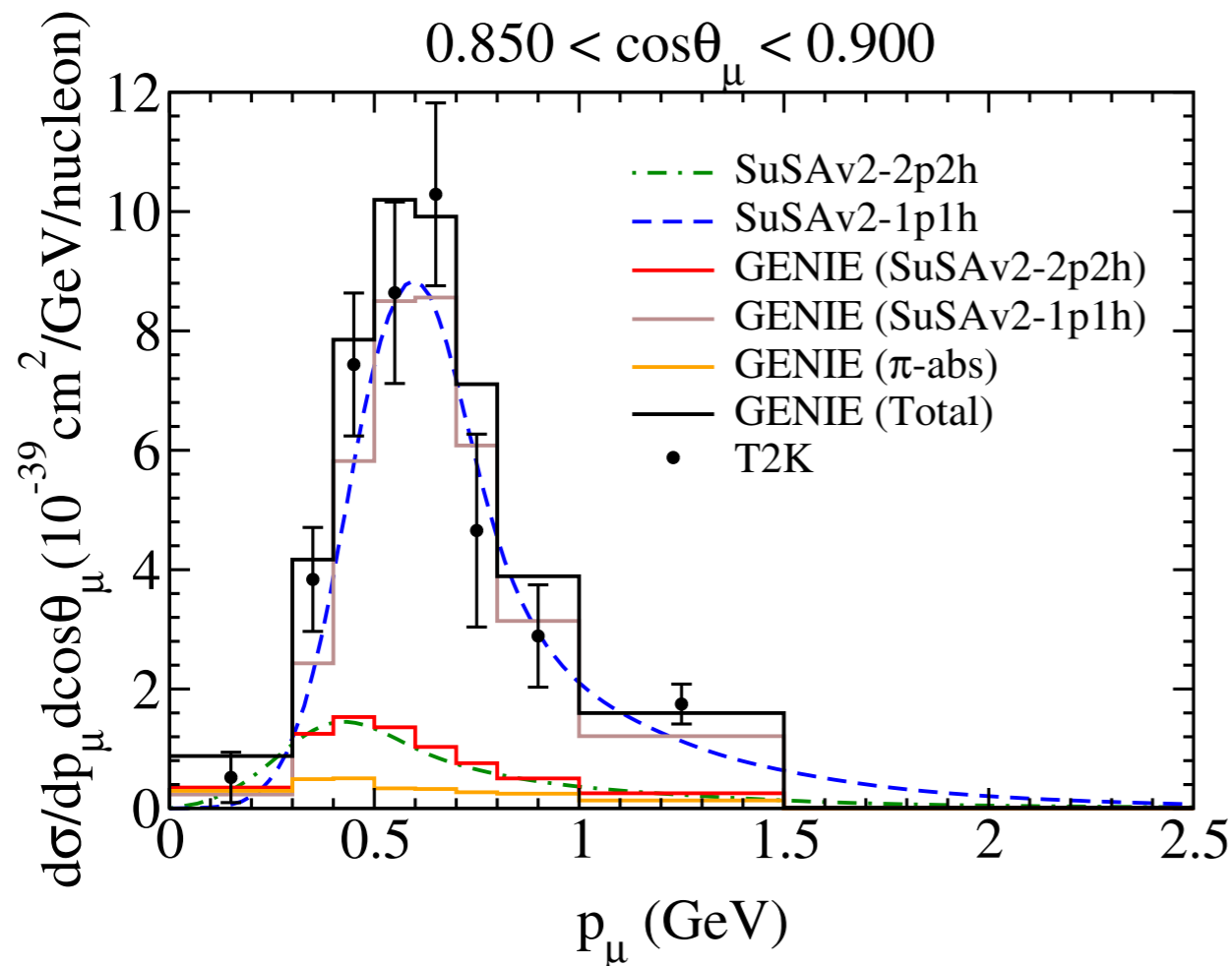
variables devised in order to enhance nuclear effects (Fermi motion, FSI, 2p2h...)

## Important nuclear effects beyond PWIA



# Implementation of SuSAv2 in GENIE (S.Dolan, G.Megias, S.Bolognesi)

S. Dolan, G. Megias, S. Bolognesi, *Phys.Rev.D* 101 (2020)



**Important differences between 2p2h models implemented in GENIE**

The SuSAv2 model was implemented from the inclusive results under some approximations. The implementation can be improved starting from the complete semi-inclusive results.

# Summary and future work

- ➔ Validation against  $(e,e')$  data is a solid benchmark for nuclear models to be used in analyses of neutrino oscillation experiments. Superscaling sets strong constraints on modeling.
- ➔ The SuSAv2-MEC model, based on RMF and including FSI and two-body currents, provides a satisfactory comparison with both electron and neutrino scattering off different nuclei (carbon, oxygen, calcium, titanium, argon).
- ➔ Computationally demanding microscopic calculations can be translated into a rather straightforward formalism, easier to be implemented in MC event generators.
  - SuSAv2 is now in GENIE (“inclusive” implementation)
  - implementation in NEUT is in progress
- ➔ Work in progress:
  - inclusive neutrino scattering including all inelasticities (resonance, “shallow”, DIS), especially relevant for DUNE
  - semi-inclusive reactions (more sensitive than inclusive to the details of nuclear models), necessary to compare with future exclusive measurements and to get more reliable implementation in MC generators

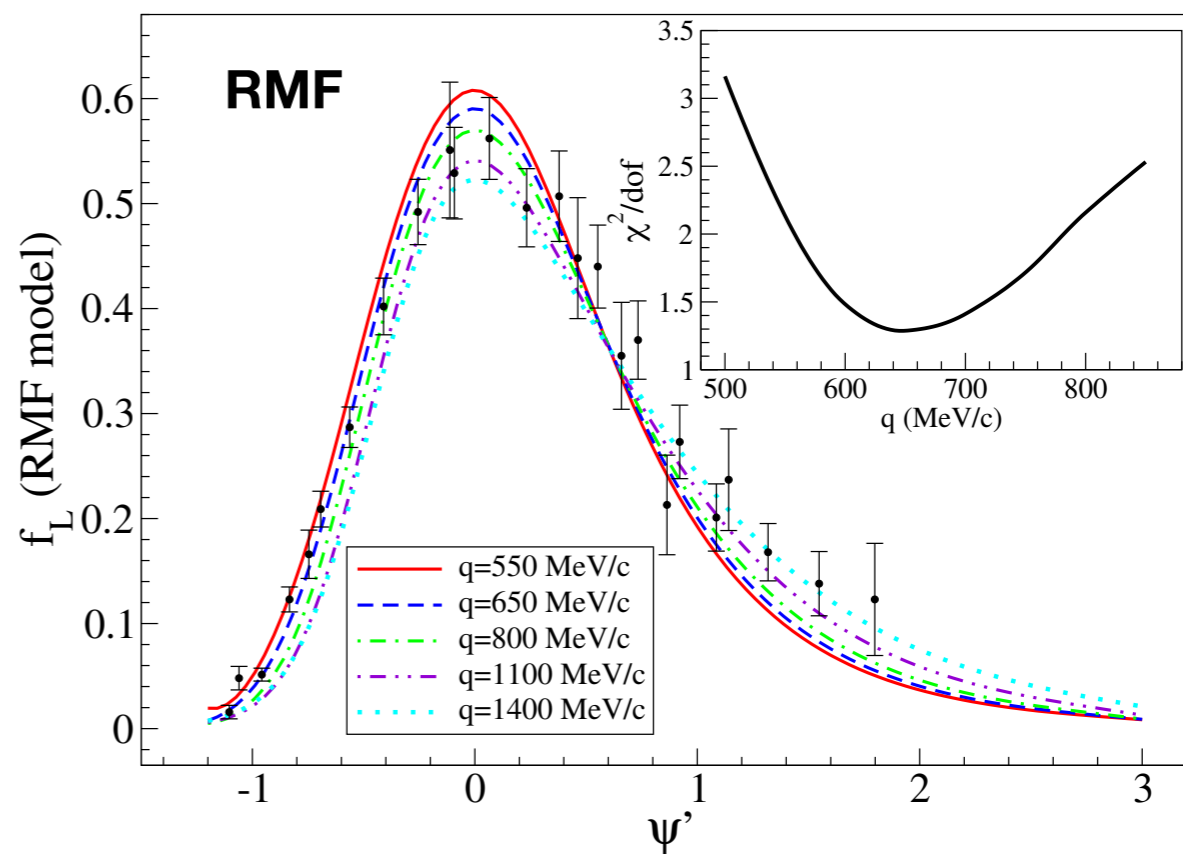
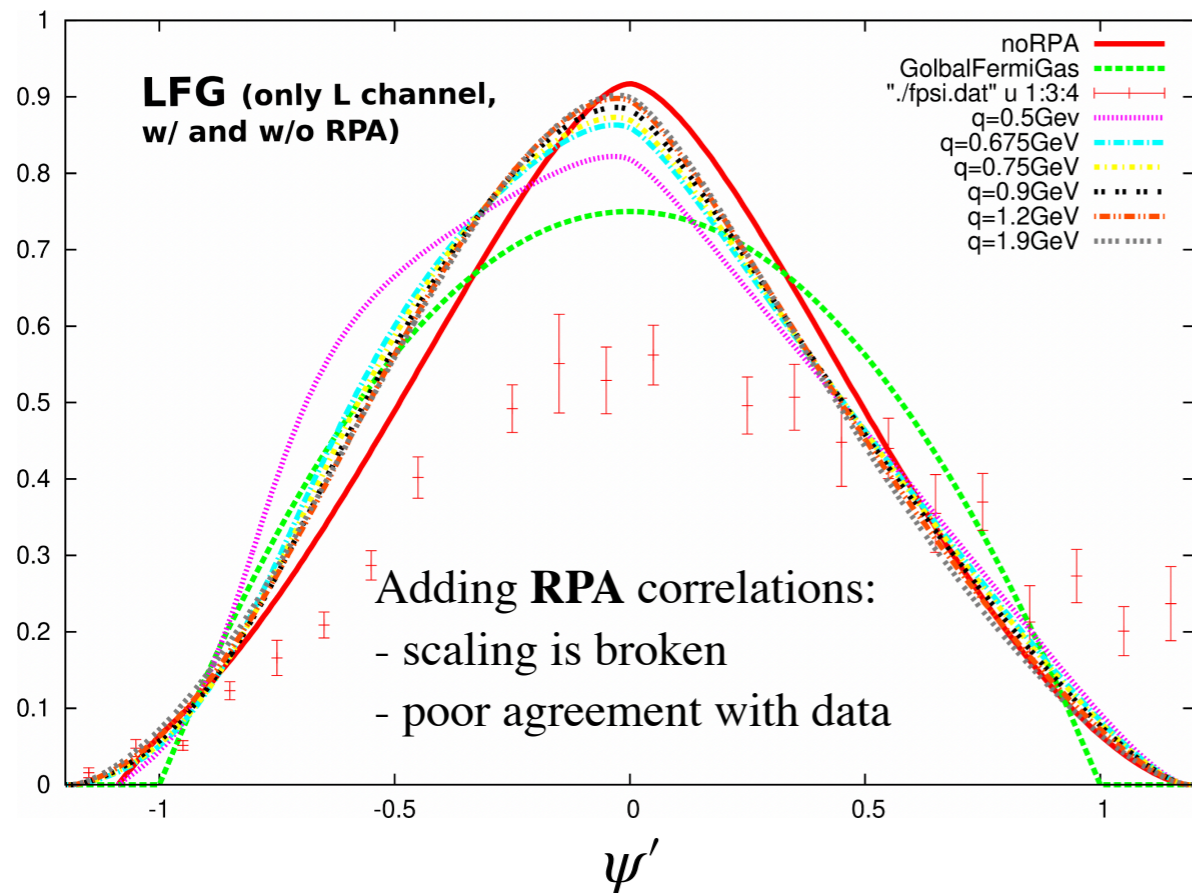
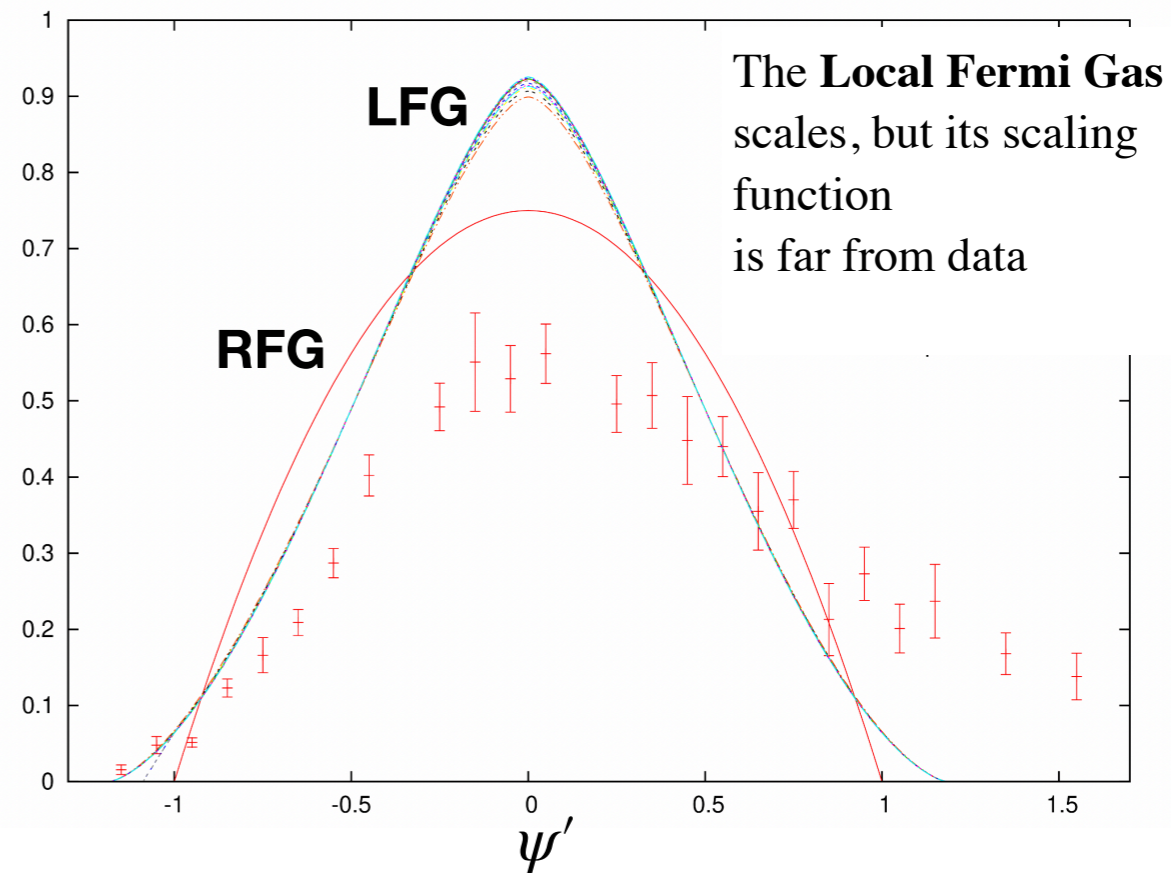
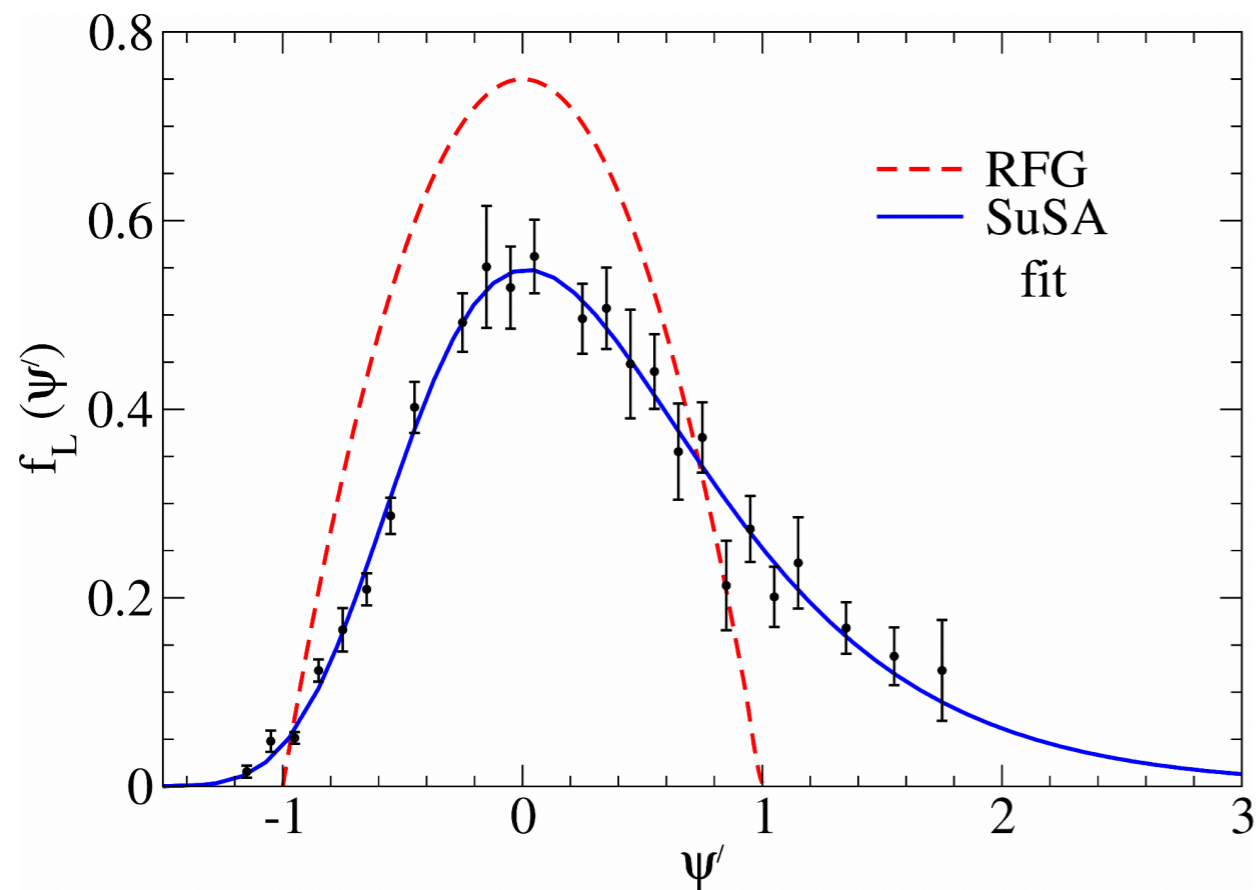
# Collaboration

- **M.B.B., A. De Pace (Torino)**
- **J.A. Caballero (Sevilla), G. Megias (Sevilla/Tokyo), J.M. Franco Patino (Sevilla/Torino)**
- **J.E. Amaro, I. Ruiz Simo (Granada)**
- **T.W. Donnelly (MIT)**
- **J.M. Udias, R. Gonzalez (Madrid)**
- **A. Antonov, M. Ivanov (Sofia)**
- **W. Van Orden (ODU & JLab)**

**Thank you**

Backup slides

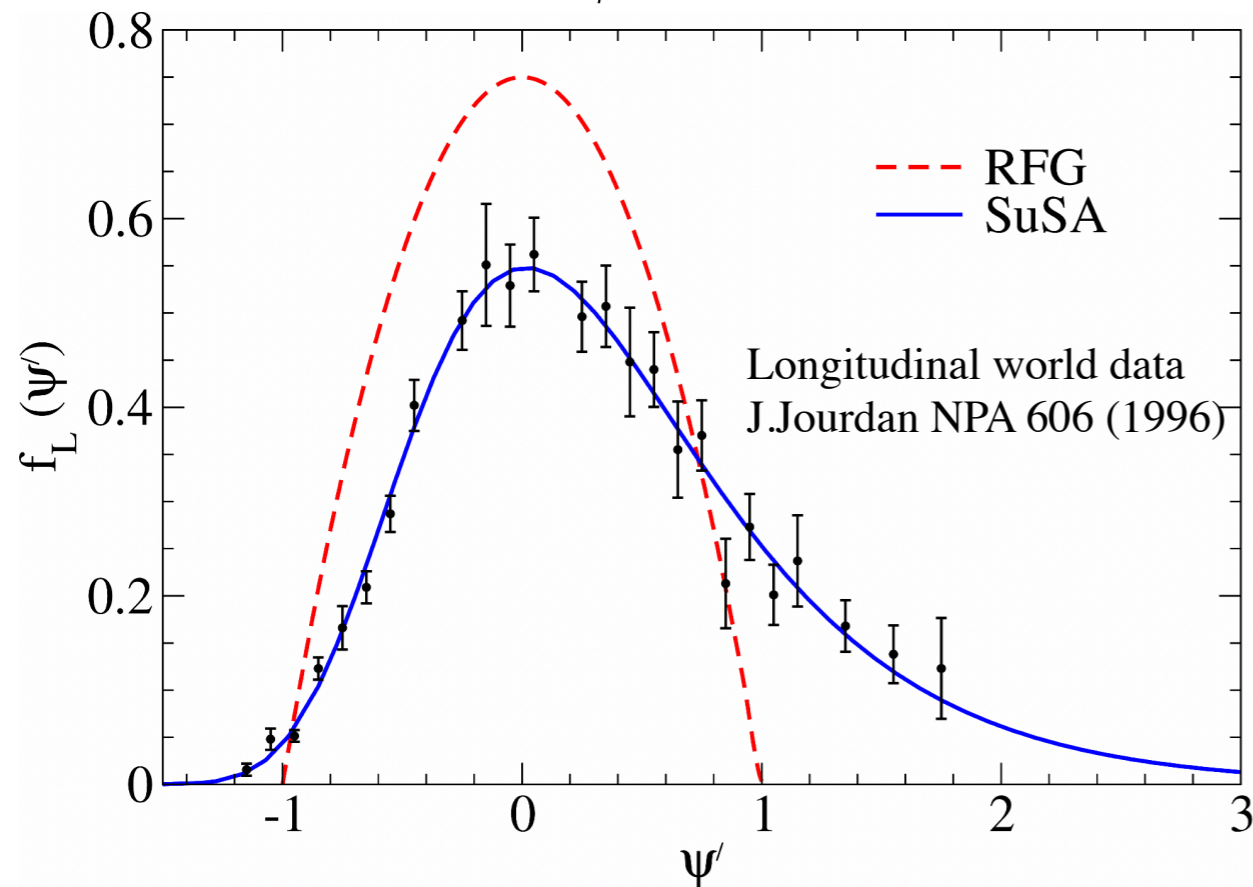
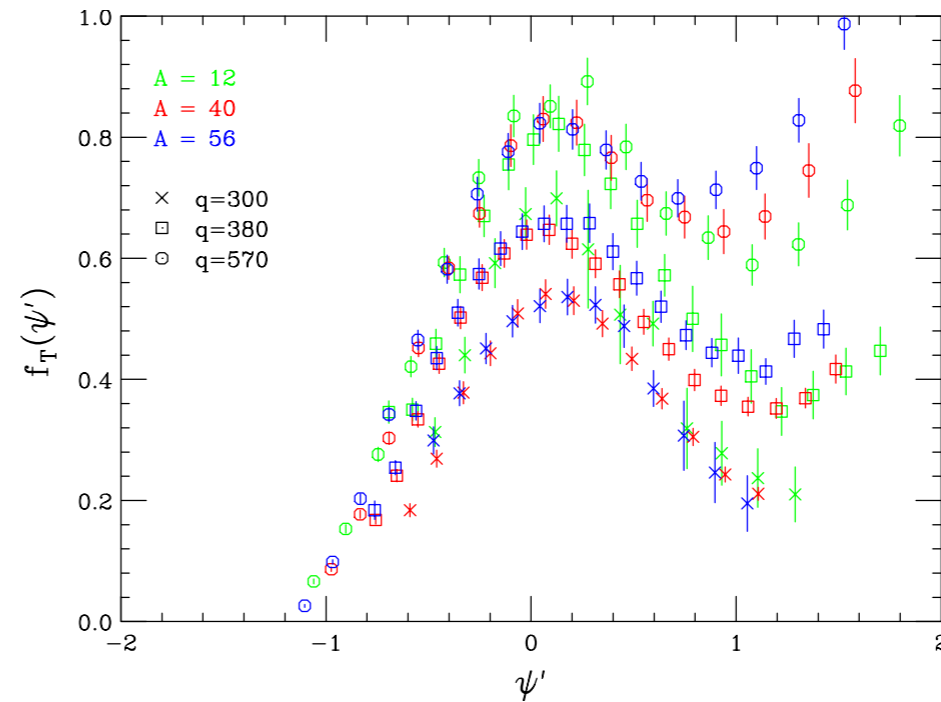
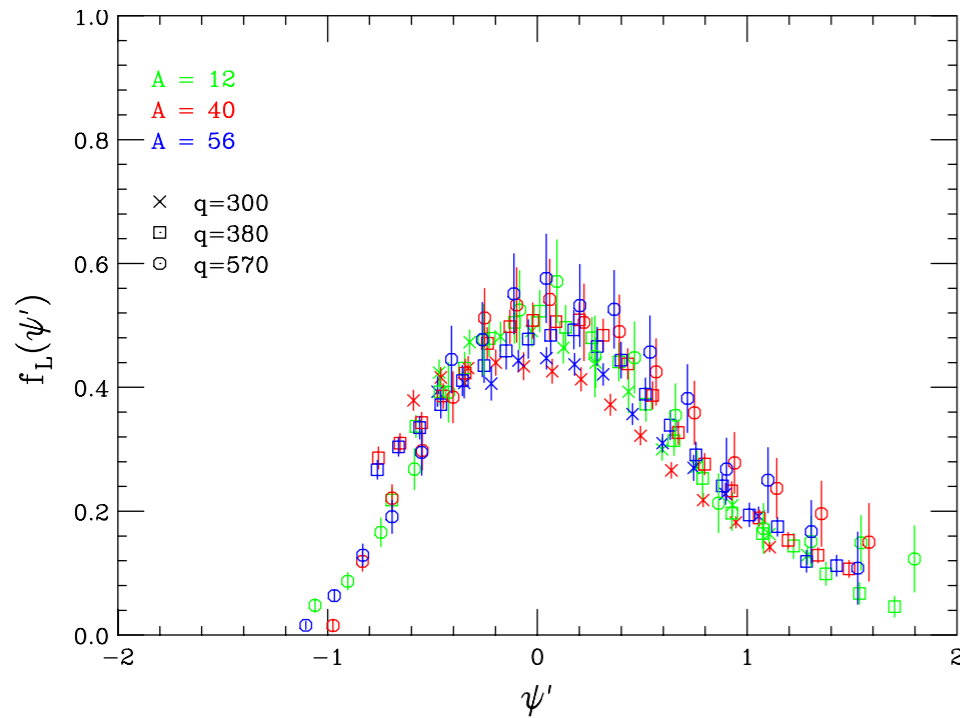
# Testing scaling for (e,e') in different nuclear models



# Longitudinal and transverse Superscaling

From L/T separated data it is found that **scaling violations** mainly occur **in the transverse channel** at  $\psi' > 0$  due to non-QE mechanisms (2p2h,  $\Delta$ ,...)

$$\hat{q} = \hat{z}$$



Stringent constraints on nuclear modeling

$$f_L^{RFG}(\psi') = \frac{3}{4} (1 - \psi'^2) \theta(1 - \psi'^2)$$

RFG very poor: overestimates the QEP by  $\sim 40\%$  and predicts a symmetric scaling function

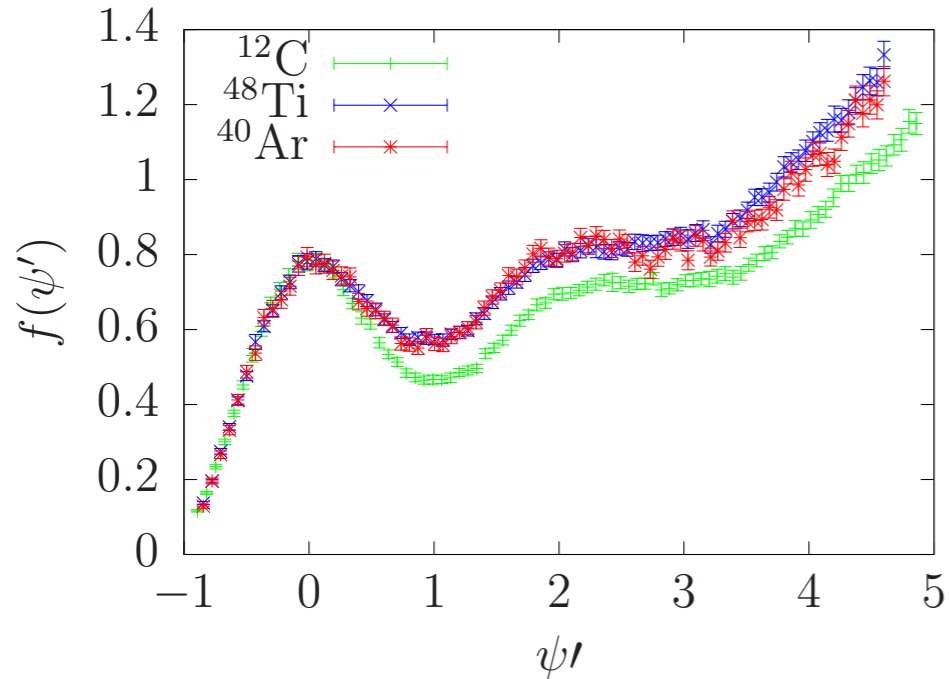
$$R^K(q, \omega) = k_F \times G^K(q, \omega) \times f(\psi')$$

$R^K$  nuclear responses  
 $G^K$  single-nucleon functions



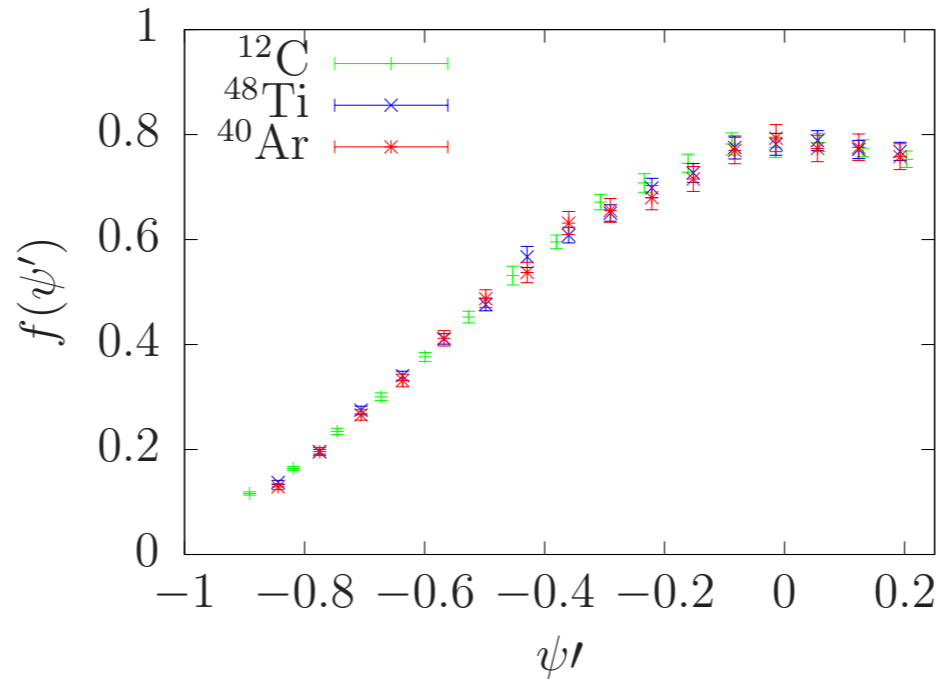
# Scaling of the inclusive (e,e') data: 1p1h and 2p2h scale differently with A

$\eta_F = k_F/m_N$  Fermi momentum



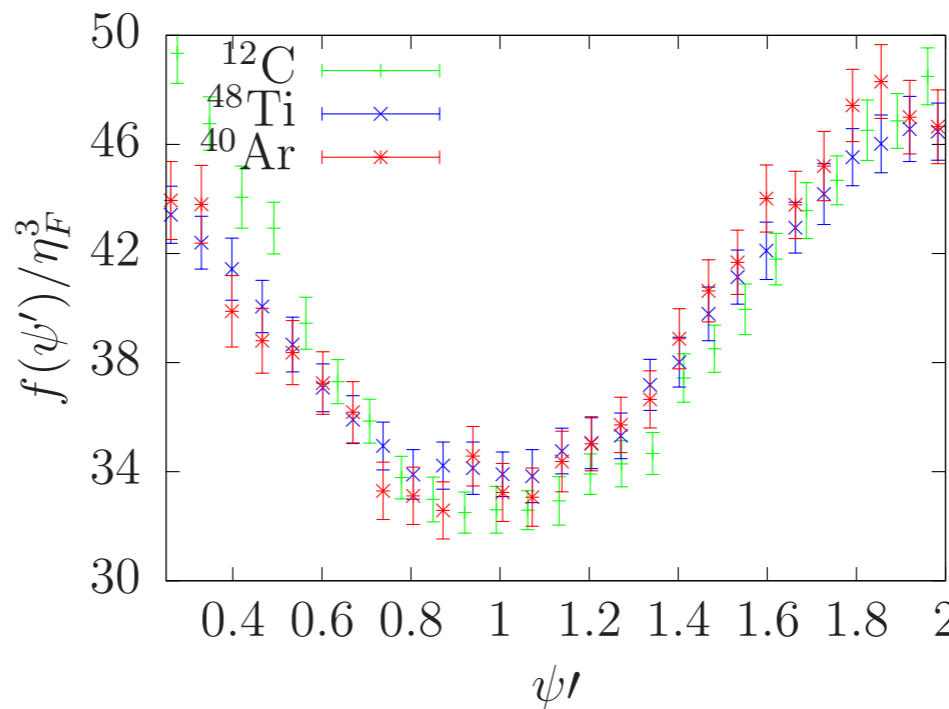
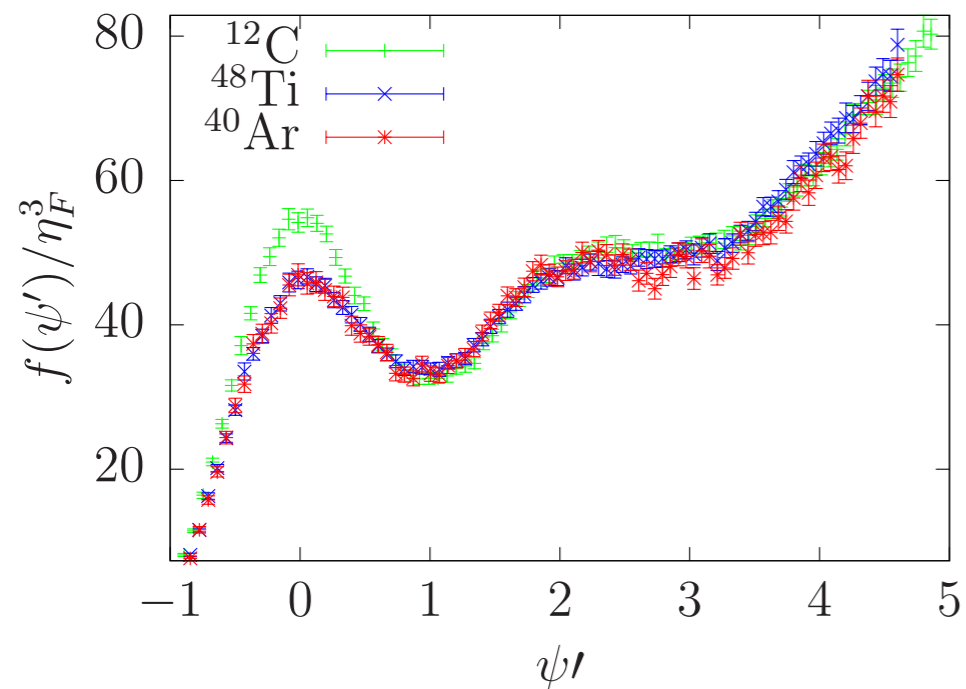
JLab (e,e') data

H.Dai *et al.*, PRC98 (2018); PRC99 (2019)



**QE region**

Ordinary second kind scaling works well:  
 $f(\psi')$  independent of  $\eta_F$   
 but it is broken in the “dip” region



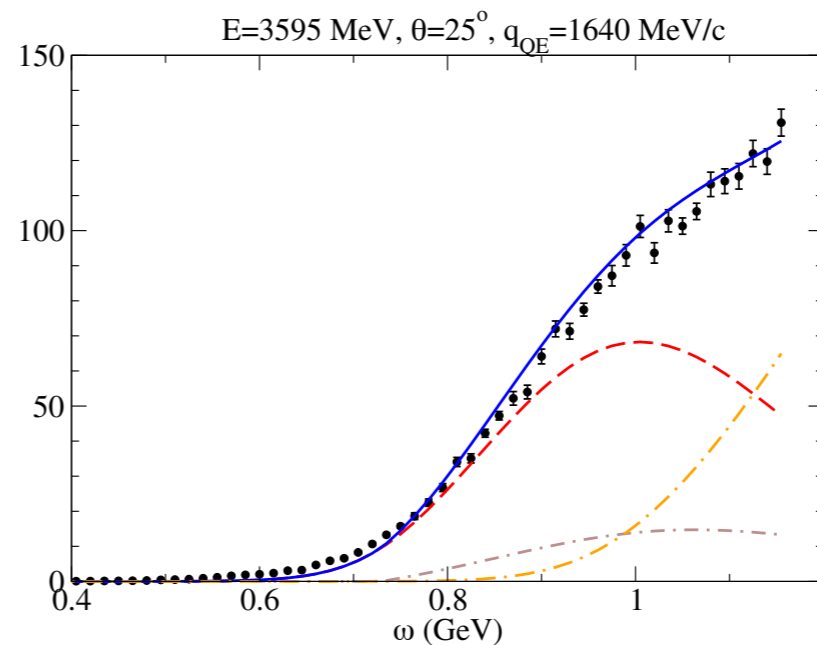
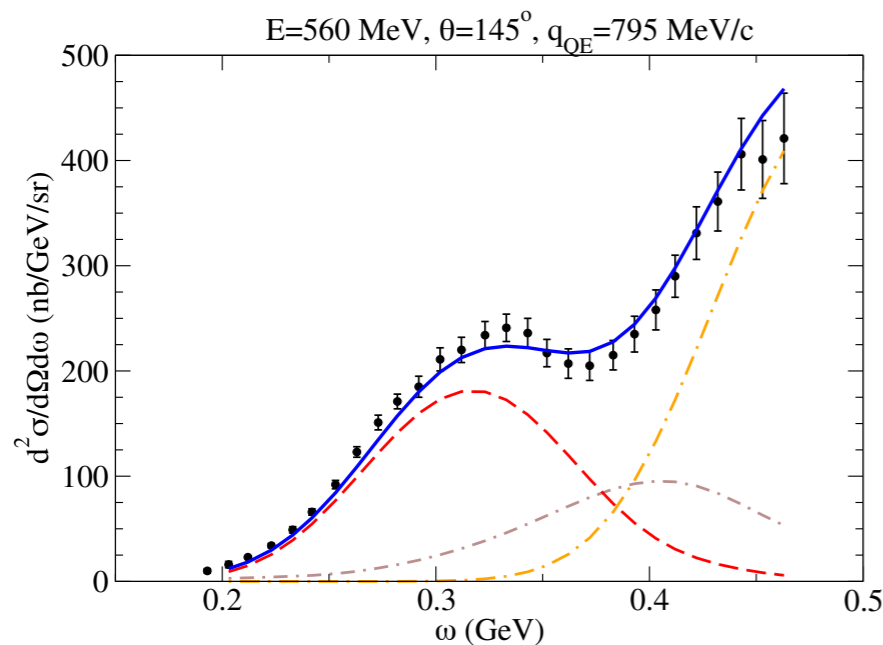
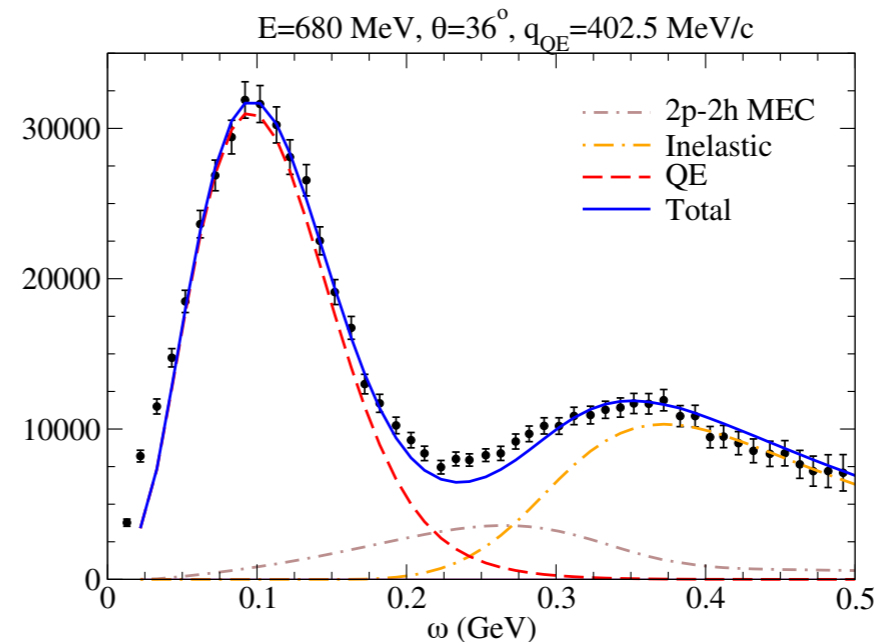
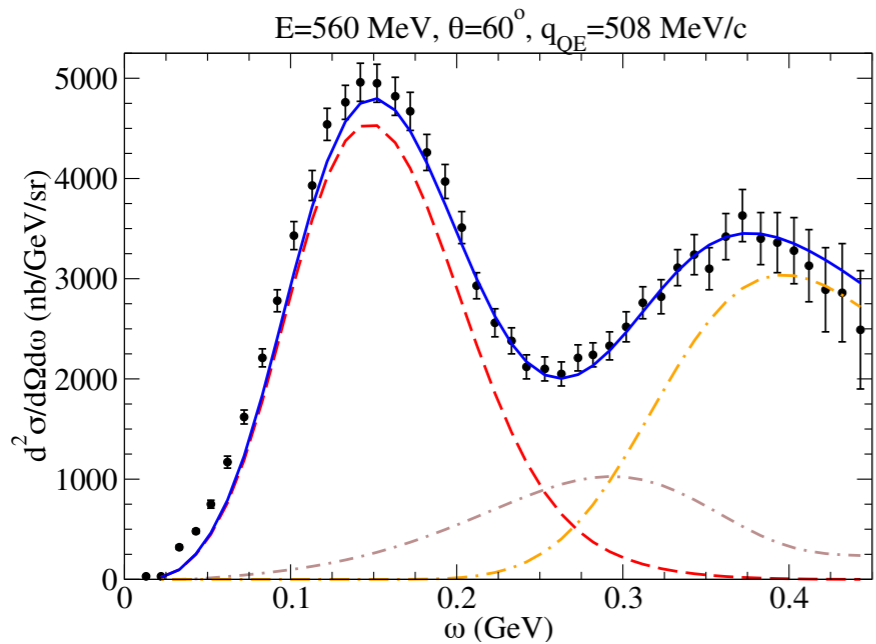
**“Dip” region**

The data scale with a different law:

$$f_{2p2h} \sim \eta_F^3$$

The same behaviour is predicted by the SuSAv2-MEC model  
 PRC95 (2017) 065502

# Validation of the SuSAv2 model : Carbon (e,e')



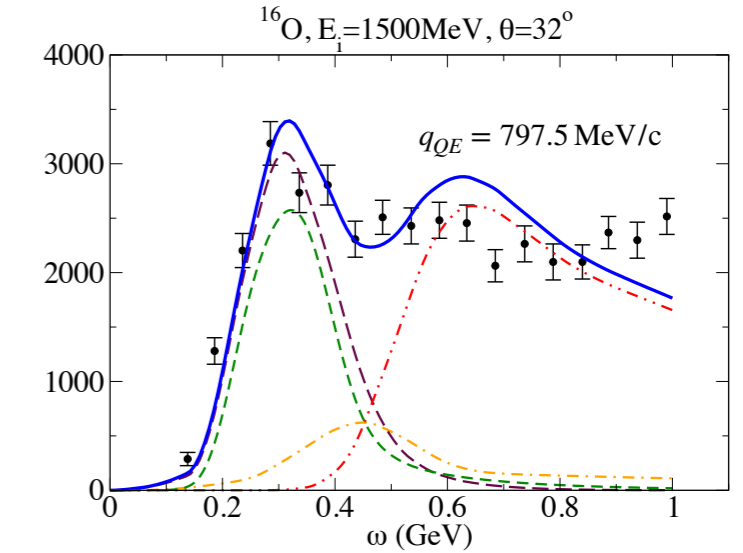
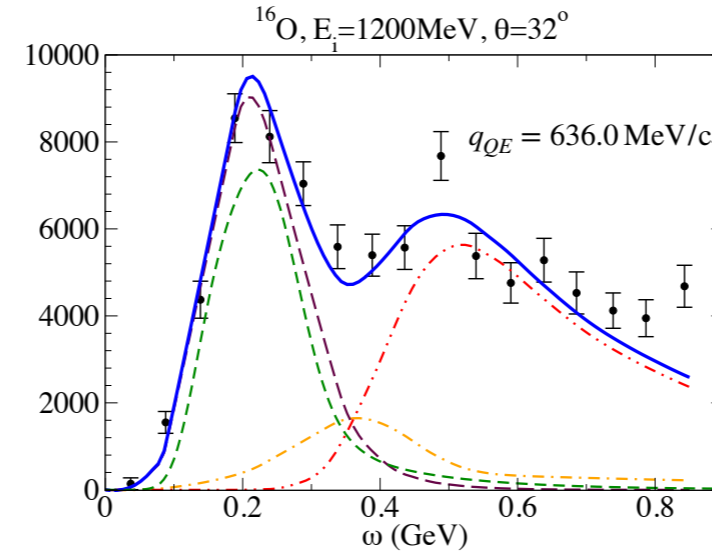
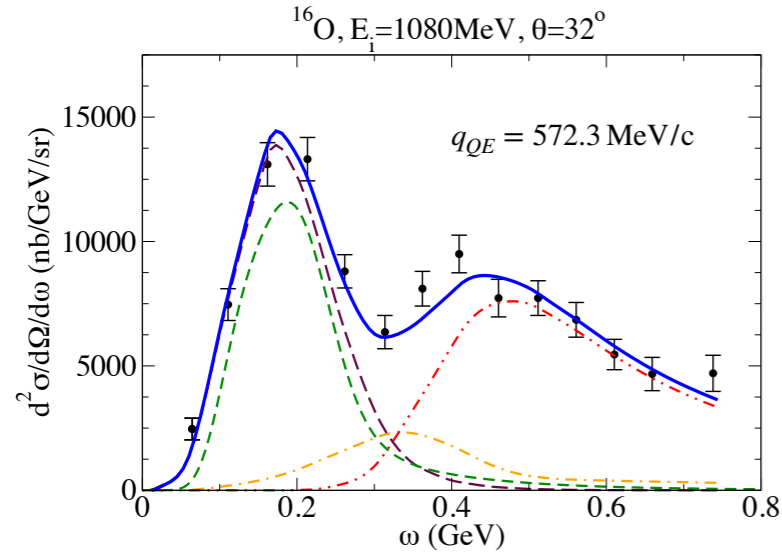
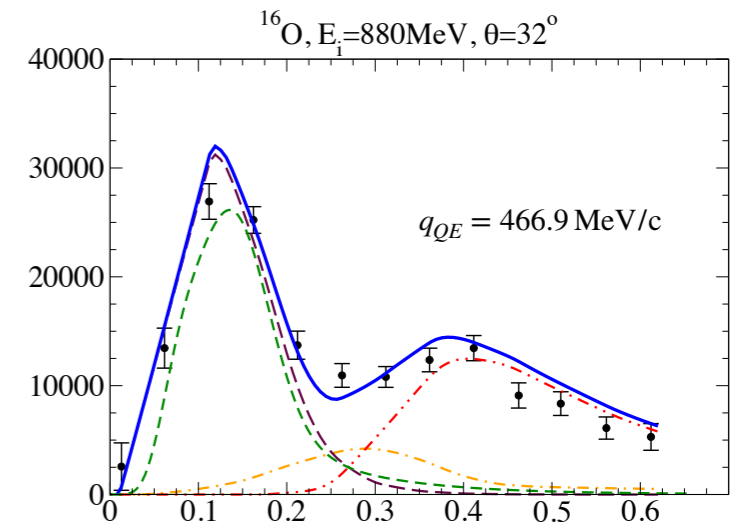
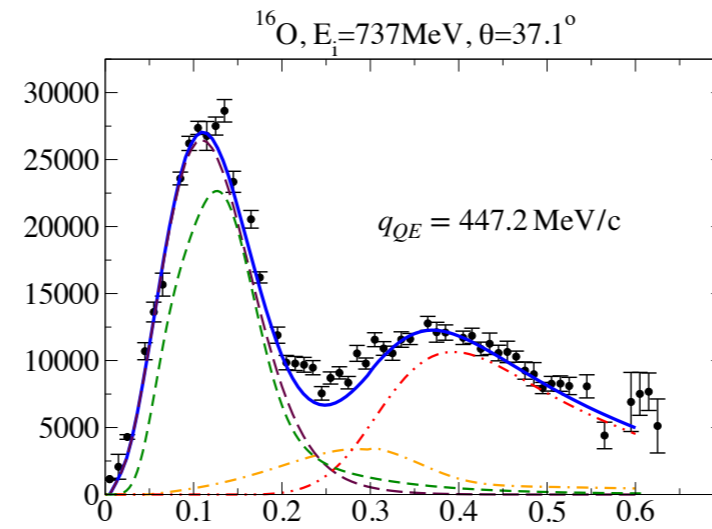
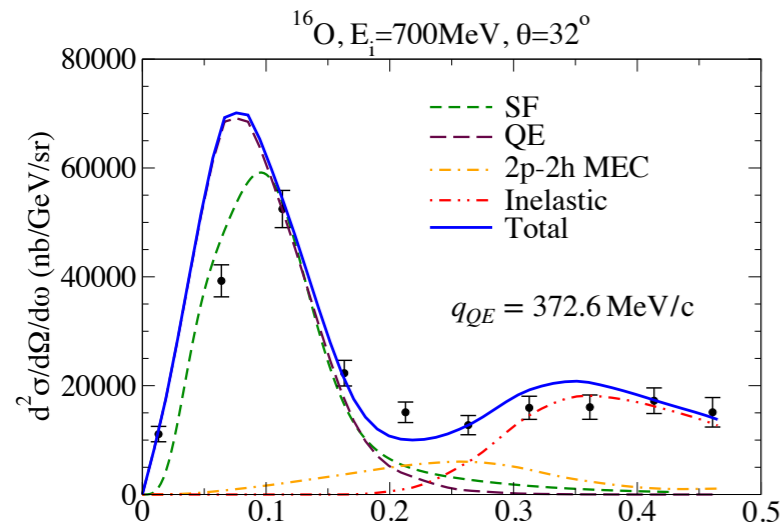
G.D. Megias *et al.*,  
PRD94 (2016)

Data:  
Barreau, NPA402 (1983),  
Day, PRC48 (1993)

The inelastic region is modelled using the Bosted and Christy parametrization of inelastic structure functions  $w_1, w_2$  and a generalisation of the scaling variable to a generic excitation:  $\psi(m_N) \rightarrow \psi(m_N^*)$

Good agreement with data in a wide kinematical region, with the exception of the very low  $q$  regime, where the superscaling approach and IA fail.

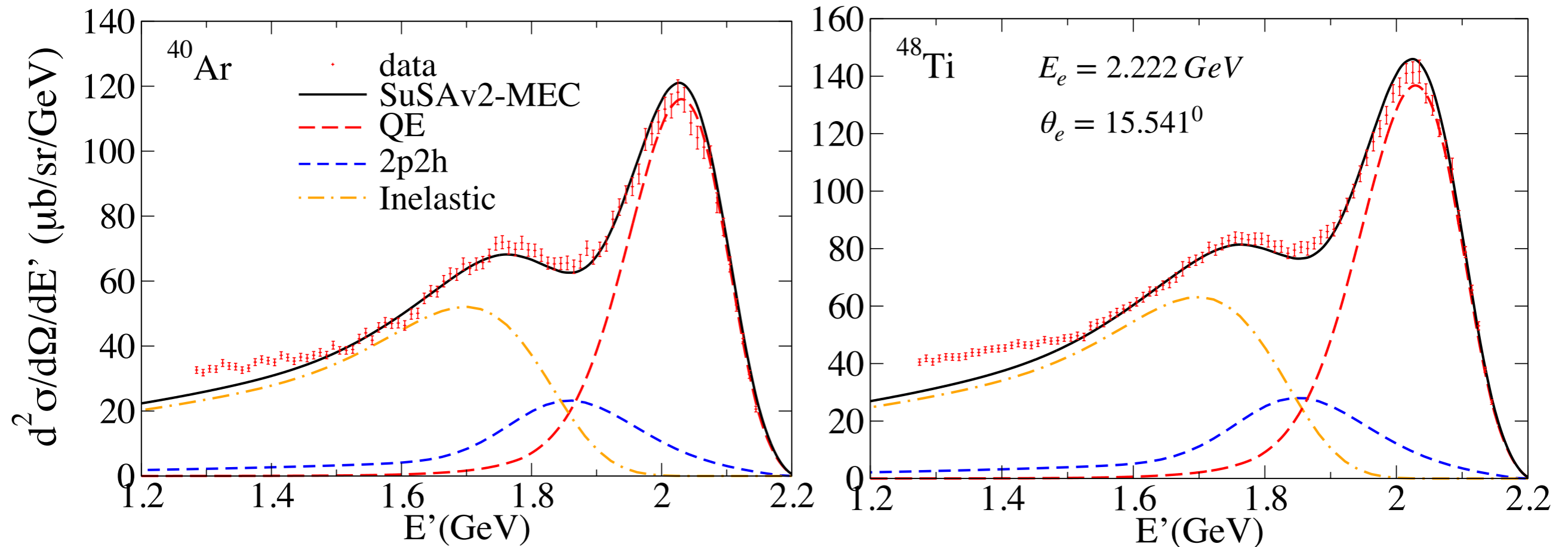
# Validation of the SuSAv2 model: Oxygen (e,e')



G.D. Megias *et al.*, JPG 46 (2019)

Data: Anghinolfi *et al.*, NPA 602 (1996), O'Connell *et al.*, PRC 35 (1987)

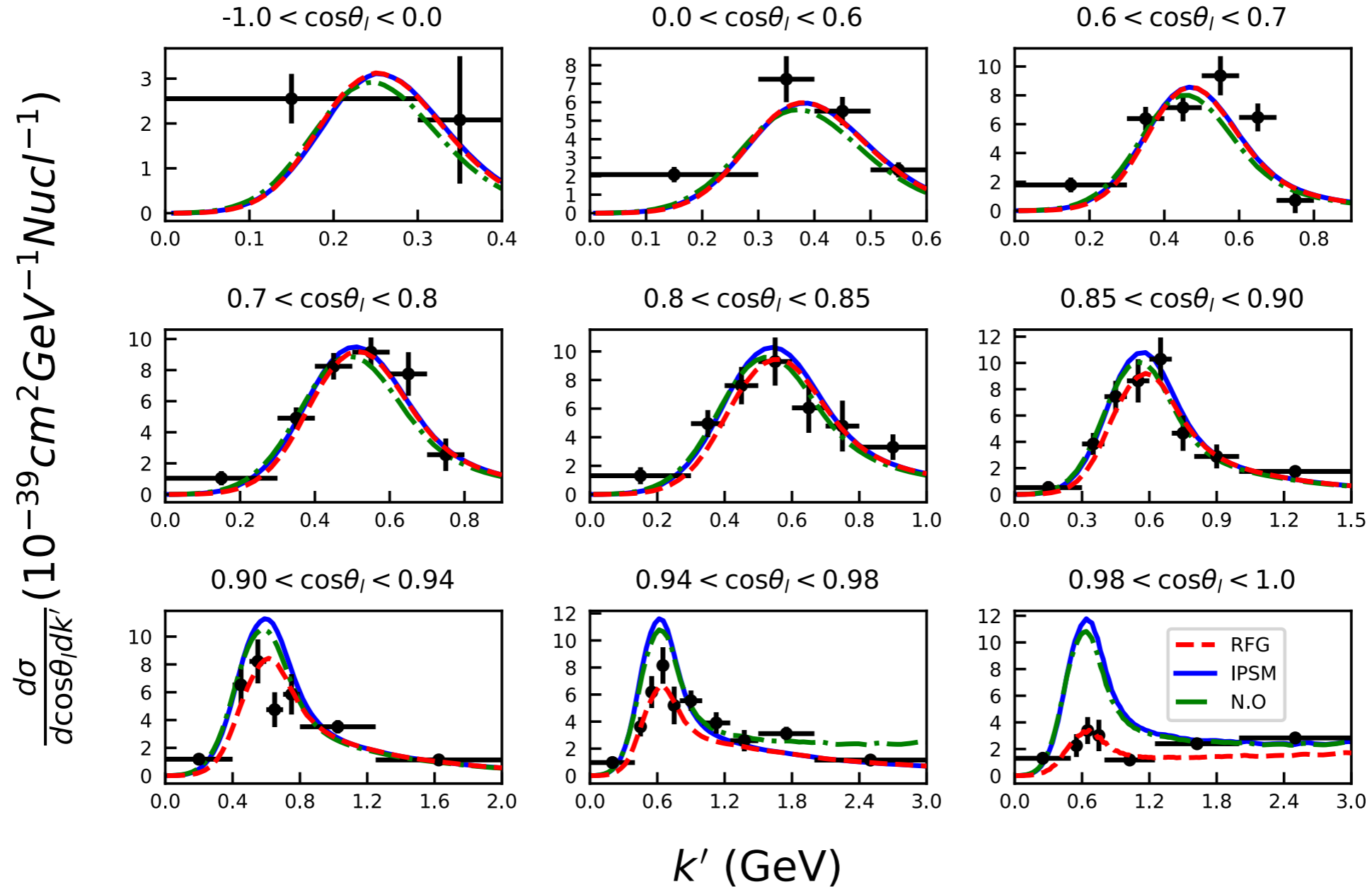
# Validation of the SuSAv2 model: Ar and Ti (e,e')



Data from H.Dai *et al.*, PRC98 (2018); PRC99 (2019)  
 JLab experiment aimed at measuring the Argon p and n spectral functions

MBB *et al.*, PRC99 (2019)

# From semi-inclusive to inclusive



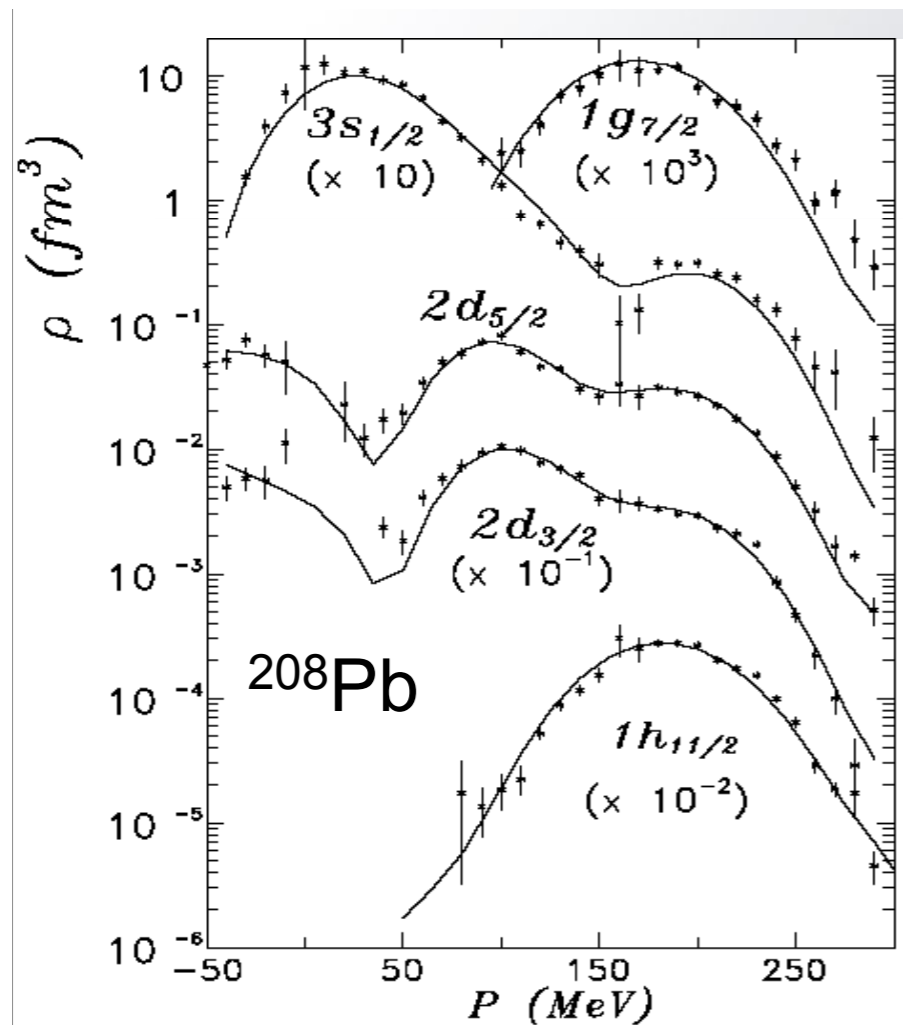
J.M. Franco Patino *et al.*, PRC 102, 064626 (2020)

Data from K. Abe *et al.* (The T2K Collaboration), PRD 98, 032003 (2018)

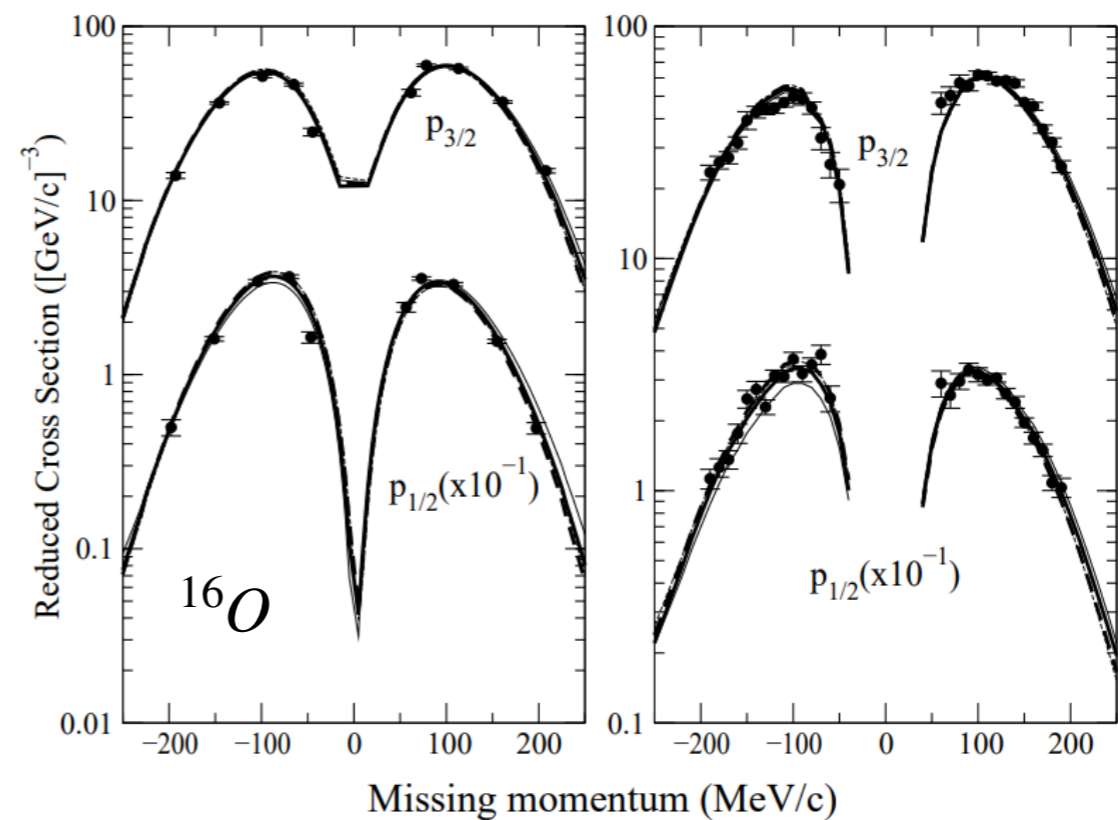
**PWIA:** at very forward angles the shell-model based approaches (IPSM and NO) suffer from lack of orthogonality between the bound and scattering wave functions.

# Relativistic Mean Field for (e,e'p)

The RMF prediction has been compared successfully to electron scattering exclusive data in the 90's



J.M. Udias et al., PRC 48, 2731 (1993)  
PRC 51, 3246 (1995)



J.M. Udias et al., PRC 64, 024614 (2001)

# Asymmetric Fermi gas

## Fermi momentum and separation energies

Asymmetric RFG for QE lepton-nucleus scattering, Phys.Rev. C98 (2018) no.3, 035501

X(A,Z,N)	$S_n$ (MeV)	$S_p$ (MeV)	$k_F^0$ (MeV/c)	$k_F^n$ (MeV/c)	$k_F^p$ (MeV/c)
C(12,6,6)	18.72	15.96	228	228	228
B(12,5,7)	3.37	14.10		240.02	214.56
N(12,7,5)	15.04	0.60		214.56	240.02
Ar(40,18,22)	9.87	12.53	241	248.23	232.17
Cl(40,17,23)	5.83	11.68		251.93	227.78
K(40,19,21)	7.80	7.58		244.41	236.39
Pb(208,82,126)	7.37	8.00	248	261.77	226.85
Tl(208,81,127)	3.79	7.55		262.46	225.92
Bi(208,83,125)	6.89	3.71		261.07	227.76

TABLE I: Neutron and proton separation energies ( $S_n$ ,  $S_p$ ) and Fermi momenta ( $k_F$ ) used in this work.

- Two effects of asymmetry:
1.  $k_F^p \neq k_F^n$       small unless  $N \gg Z$
  2.  $S_p \neq S_n$       - no effect for NC processes ( $e, e'$ ), ( $\nu, \nu'$ ): the  $p$  and  $h$  separation energies cancel in  $\delta(\omega - E_p + E_h)$
- can be large for CC scattering ( $\nu, l$ )  
even for isoscalar nuclei (C,O)